Improving Individual Tree Detection Using Drone Remote Sensing for Ecosystem Modeling Purposes

Ville Tuominen

School of Science

Thesis submitted for examination for the degree of Master of Science in Technology.

Espoo July 19, 2022

Supervisor

Prof. Antti Punkka

Advisor

Ph.D. Pavel Alekseychik

Aalto University
School of Science

Aalto University
School of Science

Aalto University, P.O. BOX 11000, 00076 AALTO
www.aalto.fi
Abstract of the master's thesis

Author Ville Tuominen

Title Improving Individual Tree Detection Using Drone Remote Sensing for Ecosystem Modeling Purposes

Degree programme Mathematics and Operations Research

Major Systems and Operations Research **Code of major** SCI3055

Supervisor Prof. Antti Punkka

Advisor Ph.D. Pavel Alekseychik

Date July 19, 2022 **Number of pages** 52 **Language** English

Abstract

Remote sensing using drones allows to analyze the state of a forest even at the level of individual trees. Data in the resolution of centimeters in which trees can be delineated can be used to design detailed harvest plans in Continuous Cover Forestry as well as to measure tree growth, health and the effect of external factors such as heat waves on the level of individual trees.

This thesis develops methods for Individual Tree Detection based on commonly used local maxima filtering algorithm using high resolution Canopy Height Model (CHM) derived from photos taken using a drone. The creation of CHM is presented by using Structure from Motion -technique. With initial estimate from the local maxima filtering, two further methods to remove incorrect tops are presented to improve the detection quality. The methods are based on inspecting the neighborhood of each top as well as comparing data sets collected before and after selection harvesting in the study site. Challenges for the methods caused by the selection harvesting are also examined.

Another novelty is the estimation of the distribution of undetected trees using a statistical method. This is needed since the drone-based CHM does not separate smaller trees under the topmost canopy layer. The parameters for the estimation are derived from field measurements, which are also used for validating the remote sensing results.

With the presented methods, a better estimation of the distribution of trees in the study site is obtained as almost all incorrectly observed trees are removed while more actual trees are detected. This distribution can be used to estimate the calculated individual crown parameters for those trees that are not detected by remote sensing, and detailed analysis on the forest ecosystem can be performed.

Keywords Drone Remote Sensing, UAV, Individual Tree Detection, Local Maxima Filtering, Continuous Cover Forestry, Multitemporal Analysis

Aalto University
School of Science

Aalto-yliopisto, PL 11000, 00076 AALTO
www.aalto.fi
Diplomityön tiivistelmä

Tekijä Ville Tuominen

Työn nimi Yksittäisten puiden tunnistaminen lennokin avulla ekosysteemien mallinnusta varten

Koulutusohjelma Matematiikka ja operaatiotutkimus

Pääaine Systeemi- ja operaatiotutkimus **Pääaineen koodi** SCI3055

Työn valvoja Prof. Antti Punkka

Työn ohjaaja FT Pavel Alekseychik

Päivämäärä 19. heinäkuuta 2022 **Sivumäärä** 52 **Kieli** Englanti

Tiivistelmä
Kaukokartoitus käyttäen lennokkeja mahdollistaa metsän tilan tarkkailun jopa yksittäisten puiden tarkkuudella. Tämänkaltaisella, parhaimmillaan muutaman senttimetrin tarkkuuksisella aineistolla, voidaan luoda yksityiskohtaisia harvennussuunnitelmia jatkuvapeitteisessä metsänhoidossa. Myös puiden kasvun, terveydentilan sekä ulkoisten tekijöiden kuten helleaaltojen vaikutuksen tutkiminen on mahdollista yksittäiset puut erottelevassa aineistossa.

Tässä työssä parannetaan menetelmiä, joilla löydetään yksittäisten puiden sijainnit lennokilla otettujen valokuvien pohjalta tuotetusta tarkasta latvusmallista. Tätä varten esitellään latvusmallin tuottaminen käyttäen Structure from Motion -menetelmää. Puiden sijaintien etsiminen pohjautuu paikallisten huippujen löytämiseen latvusmallista, ja työssä esitellään useita menetelmiä virheellisten pisteiden tunnistamiseksi käyttäen hyödyksi tietoa löydettyjen huippujen ympäristöstä sekä vertailua kahden ajallisesti eri aikaan tuotetun aineiston välillä. Työssä tutkitaan myös minkälaisia vaatimuksia aineistojen tallentamisen välillä tutkimusmetsässä suoritettu harvennushakkuu asettaa menetelmille.

Koska valokuviin pohjautuva latvusmalli ei erottele korkeimpien puiden alle jääviä puita, käytetään työssä kenttätutkimuksia hyödyntävää uutta tilastollista menetelmää puiden kokonaismäärän arvioimiseksi. Kenttätutkimuksia hyödynnetään myös käytettyjen kaukokartoitusmenetelmien tulosten arvioimiseen.

Esitetyillä menetelmillä saadaan vertailutasoa tarkempi arvio puiden määrien jakaumasta tutkimusalueella, sillä väärin puiksi merkittyjen pisteiden määrää vähenee selvästi ja oikeiden havaintojen lukumäärä kasvaa. Tarkemman jakauman avulla yksittäisille puille lasketut parametrit voidaan estimoida myös niille puille, joita ei ole havaittu käyttäen kaukokartoitusmenetelmiä, ja koko metsäekosysteemin tilaa voidaan analysoida aiempaa tarkemmin.

Avainsanat kaukokartoitus, yksittäisten puiden havaitseminen, latvusmalli, jatkuvapeitteinen metsänkasvatus

Contents

Abstract **2**

Abstract (in Finnish) **3**

Contents **4**

Acknowledgements **6**

Abbreviations **7**

1 Introduction **8**

2 Background **11**
2.1 Optimization in forest management 11
2.2 Climate change affecting decision making 12
2.2.1 Continuous Cover Forestry 14
2.3 The utilization of remote sensing data 15
2.3.1 Object-based analysis 16
2.3.2 Species classification 16
2.3.3 Thermal analysis 17
2.4 The purposes of this research 17

3 Materials and Methods **18**
3.1 Data obtaining and the study site 18
3.2 Point cloud pre-processing 19
3.3 Finding tree locations 22
3.4 Branch top removal 22
3.5 Clustering and filtering tops using temporal data 24
3.5.1 Temporal Clustering 24
3.5.2 Filtering tops using clustering 25
3.6 Generating temporal top pairs 25
3.7 Crown segmentation 27
3.8 Estimating the total number of trees 28

4 Results **30**
4.1 Point cloud processing 30
4.2 Tree top locations 32
4.2.1 Branch Top Removal 33
4.2.2 Temporal Clustering and top pairs 34
4.3 Results and validation to field data 35
4.4 Estimating the total number of trees 37
4.5 Crown segmentation 39
4.5.1 Top pairs using Intersection Method 40
4.5.2 Calculating tree parameters 41

5 Discussion **43**
5.1 Remote sensing . . . 43
5.2 Individual Tree Detection and Segmentation . . . 43
5.3 Applicability for decision making and ecosystem modeling . . . 45

6 Conclusion **46**

References **48**

Acknowledgements

It is worth noting that the pre-processing in Chapter 3.2 is based on workflow developed by Mitro Müller. The Individual Tree Detection for the Terrestrial Laser Scan data used in Chapter 4.3 is performed by Timo Pitkänen. The process for estimating the number of hidden trees in Chapter 3.8 was introduced by Lauri Mehtätalo.

This study was co-funded by the Strategic Research Council (SOMPA project, decision no. 336570) and the Academy of Finland Flagship Programme (UNITE flagship, decision no. 337655).

I would like to show my deepest gratitude to Pavel Alekseychik for supervising my thesis, supporting my work and for the field trips. I would also like to thank Lauri Mehtätalo, Antti-Jussi Kieloaho, Jonathan Atherton, Mitro Müller and Timo Pitkänen for their support in methods. I would also like to mention Mikko Peltoniemi, Anne Ojala and Raisa Mäkipää from Luke for their support and for giving the possibility to write the thesis. Thanks to all Luke 2021 trainees for the moments at both Viikki and Ränskälänkorpi.

As this thesis completes my studies at Aalto, I would like to show my deepest gratitude to the Otaniemi student community. I would like to thank numerous people especially in Fyysikkospeksi, OUBS, Teekkarispeksi and the Guild of Physics for giving me the most memorable moments and the possibilities to do amazing things with other people. Thanks to all my friends who have supported me during my student years. I would also like to thank Professor Antti Punkka from Aalto for supporting me throughout my studies.

1.5.2022

Ville Tuominen

Abbreviations

ALS Aerial Laser Scanning

CCF Continuous Cover Forestry

CHM Canopy Height Model

DN Digital Numbers (uncalibrated pixel values)

DAP Digital Aerial Photogrammetric point cloud

DEM Digital Elevation Model

DTM Digital Terrain Model

GCP Ground Control Point

ITD Individual Tree Detection

ITS Individual Tree Segmentation

LMF Local Maxima Filtering

NDVI Normalized Difference Vegetation Index

NGRDI Normalized Green-Red Difference Vegetation Index

NIR Near-Infrared spectral channel

SfM Structure from Motion

TLS Terrestrial Laser Scanning

UAV Unmanned Aerial Vehicle (here drone)

1 Introduction

As key sustainability issues, such as climate change, biodiversity loss and nutrient loading, become increasingly severe, more detailed and recent data on ecosystem status is needed to support policy making. *Remote sensing* — the usage of satellites, planes, helicopters, and drones to capture information from distance — enables fast and timely collection of data which is instrumental in addressing these issues.

Remote sensing data representing the state of vegetation and soil is valuable for agricultural and forestry management planning. It extends traditional labor-intensive field measurements with instantaneous spatial view of surface conditions and expands the small study sites with larger areas. For some variables, it can be used to derive useful proxies of various vegetation and soil traits measured in-situ (Dainelli et al., 2021). In the context of forestry, forest inventories as well as the monitoring of regeneration success and tree health are the main use cases of remote sensing (Surový et al., 2019).

Besides decision making, remote sensing can be used for detailed research on forest *ecosystem modeling*. Ecosystem modeling aims to model dynamics between various physiological variables and understand the feedbacks between weather, climate, vegetation, and soil. In a changing climate, the interconnected and complex systems in nature may have unexpected reinforcing and balancing feedback-loops that can speed up or down climate change effects (Sebestyén et al., 2021). For example, extreme heatwaves caused by increased temperatures can result in reduction of gross primary production leading to high releases of carbon dioxide (Friend et al., 2005) that further accelerate climate change.

Using *Unmanned Aerial Vehicles* (UAVs), such as drones, highly detailed remote sensing of nature is possible. Equipped with different types of cameras and laser scanners, UAVs provide spectral and structural remote sensing data with such a high resolution that individual trees can be detected and inspected. Previously, with satellite or plane remote sensing, only forest-level details could be obtained (Dainelli et al., 2021). UAVs equipped with traditional RGB cameras, as well as thermal, multispectral, or hyperspectral sensors produce remote sensing data that can be used to analyze tree health, reveal infectious diseases in plants and separate different tree species (Surový et al., 2019). As an example, the response to extreme weather such as droughts and heat weaves can be studied on individual tree level.

Information on the tree crown structure can be obtained from standard photos using technique called *Structure from Motion* (SfM, Schonberger et al., 2016). While airborne and terrestrial laser scanners have been popular due to their extremely high resolution, similar 3D models can also be constructed using SfM. This can be done with much lower equipment cost and easier processing than laser scanning whilst retaining sufficient quality on output. In the case of forestry, it is possible to construct a 3D model of the canopy with resolution more than 5 cm by taking overlapping photos using a consumer-grade camera during a drone flight on a constant altitude above forest.

Precision forestry such as *Continuous Cover Forestry* (CCF) can benefit from the details of individual tree parameters, such as tree height, stem volume and species, to provide sustainable forest management strategies (Wulder et al., 2008). CCF maintains continuous uneven-aged forest structure to provide more resilience to varying conditions and stable economic output, although it requires more frequent management interventions than traditional clear-cut approach (e.g. Gaulton, 2010).

Especially in the context of drained peatlands forests, optimizing the harvesting in CCF and thus the growth of new trees by selecting trees by their size, health and age can have significant effects on the soil emissions. In managed peatlands, the water table depth in the ground is managed using ditches and by retaining a proportion of larger trees. Lowering water table level boosts tree growth but allows the peat to decay as CO_2. On the contrary, rising water level increases the production of CH_4, which is much stronger greenhouse gas than carbon dioxide. The peatland forests are responsible for approximately 3% of the global anthropogenic emissions (Evans et al., 2021).

To be aware of these types of systemic effects, knowing the consequences of management decisions by having a good understanding of the forest ecosystems is important. For Continuous Cover Forestry, remote sensing data can be used to both analyze the effects of harvesting as well as to generate detailed harvesting plans that sustain environmental and economic value.

This thesis has three main goals: 1) present an end-to-end process for drone remote sensing for decision making and ecosystem modeling purposes 2) develop two methods for *Individual Tree Detection* (ITD) by extending the commonly used *local maxima filtering* (lmf) algorithm so that incorrectly detected trees are removed 3) estimate the distribution of all trees from the proportion of trees that has been detected by the remote sensing.

As an example of modern remote sensing, workflow for capturing and processing drone imagery using Structure from Motion into photogrammetric 3D *point cloud* and *Canopy Height Model* (CHM) is presented. As final product, each individual tree crown is delineated from the data. With multi-band information from the RGB, multispectral and thermal sensors, statistics are calculated for each crown. The drone flights are performed before and after selection harvesting in September 2020 and July 2021 at Ränskälänkorpi study site located in Asikkala, Finland. This dataset allows a wide range of analyses of the effects of selection harvesting (sometimes referred as partial harvesting).

For developing Individual Tree Detection, two methods to remove incorrectly detected trees are presented. ITD is initially based on local maxima filtering, which finds apex points (tree tops) that correspond to the tree trunk locations in the Canopy Height Model. As we also want to correctly find trees with smaller crown size, a small search window needs to be used. This results in an increase of incorrect tree tops, detected for example in branches. Here “Branch Top Removal” is used to remove incorrect tops by inspecting the neighborhood of each top. However, this method is not suitable for the smallest crowns and areas affected by noise. With "Temporal Clustering", ITD data from the previous year can be used to cluster the incorrect tops as points corresponding to the same tree. When these two methods are used to remove incorrect tops, the number of false positives decreases significantly while more correct tops are detected.

As only the tallest trees are visible in the drone images, smaller trees are left undetected. Statistical modeling based on field measurements can be used to supplement the remote sensing data. For estimating the total number of tops in the study area, novel Horvitz-Thompson -like estimator developed by Kansanen et al. (2016) is used. This estimates the distribution of all trees in the forest.

With the availability of multiple spectral data types from two different dates and by using the methods presented in this thesis, more detailed analysis on the forest state can be performed than previously using remote sensing data. This work is part of research that studies tree response to a severe drought period.

This thesis starts with an overall look into remote sensing and decision making in forestry in Chapter 2 with the focus being on the climate change context. In Chapter 3, data capturing and the used methods for Individual Tree Detection and Segmentation are presented. It also presents the developed methods to improve the tree detection and segmentation results, and the statistical model used to estimate the number of undetected trees.

Chapter 4 includes the results and quality assessment for the individual tree detection and tree number estimation, and the calculation of the individual tree parameters. Chapter 5 discusses possible improvements and alternative methods, as well as the application possibilities for the results. Chapter 6 summarizes the contents.

2 Background

In this section, literature related to the work in this thesis is presented. First, a general look into decision making in forestry is taken focusing on utilization of optimization methods especially in the context of climate change. After that, example use cases of remote sensing and possible methods to process the data are examined, as well as background on using remote sensing data in Continuous Cover Forestry. Finally, the motivation for this research is presented.

2.1 Optimization in forest management

The idea of sustainable forest management is to maintain the income of forestry products and preserving the aesthetics, biodiversity, and nature systems over time. Understanding the ecosystem dynamics — how the forest behaves over time with the planned actions — is crucial since the decisions such as harvesting affect the forest system state for decades. With current rapidly changing climate system, the need for understanding and predicting the behavior of ecosystems under different decisions is crucial (Surový et al., 2019).

To make decisions in forestry, having detailed current data through field measurements or remote sensing is crucial. Forest managers have mentioned the following information needs for decision making: mapping of geometrical borders of homogeneous areas (e.g. plots under different harvesting regimes), monitoring the growth of saplings, assessing height of the trees, evaluating other inventory parameters (e.g. stem volume or diameter at breast height), species classification and determining the tree health status and mortality (Surový et al., 2019). These parameters can be evaluated either at stand or individual tree level.

The review by Kaya et al. (2016) presents different attempts to optimize forest management by making decisions on, for example, whether to harvest a tree or a stand or let it grow, what kind of treatment is being applied and when the management activities should be performed. Production capacity, social aspects and environmental outcomes are assessed on a larger scale. Most of the optimization problems focus on maximizing the perceived benefit using Net Present Value (NPV) commonly using linear, mixed integer or dynamic optimization in addition to genetic algorithms and heuristic models. In the optimization models, the objectives and constraints are defined by modeling decisions' effects to the tree growth and the reactions of economic, social, and environmental systems to the actions. Optimization can be performed on either *tree-*, *stand-*, *forest-* or *landscape-level*, where the landscape refers to e.g. county on which the forests have multiple owners. Different time scales are also considered, ranging from short-term *operational planning* including e.g. worker allocations to longer *tactical planning* which includes realizations of goals set at the longest *strategic planning* level. The future improvement of these optimization models focuses on inclusion of non-commodity outcomes, such as water quality, wildlife habitat and ecological health, into the models.

In operational planning, practical decision problems are most commonly related to deciding which areas to harvest and how to cut the stems, how to build roads in the forest to carry the stems using skidders or tractors and how to route the trucks carrying the stems into the desired destinations. In addition to profit, objectives can also focus on preserving nature: selecting reserved areas for each protected species, constraining harvest so that no adjacent areas are harvested at once and analyzing the movement of wildlife species over time. To assess uncertainty caused by e.g. varying prices, stochastic models such as Markov decision models, scenario analysis and stochastic dynamic programming can be applied (Weintraub et al., 2006).

As an example, Pukkala et al. (2012) utilize stochastic adaptive optimization to find optimal adaptive harvesting strategies when wood price and forest growth are stochastic. Here the word *adaptive optimization* is used for rules that react to the current state of the nature and markets, while *anticipatory optimization* provides pre-defined plan with e.g. fixed harvesting intervals. The adaptive rules were found to provide clearly higher NPV values than the anticipatory plans. However, it was found that the timber price is a more important factor than the forest growth rate when deciding the harvest time. Additionally, having a wide variety of different tree species provides more flexibility for varying prices per species and changing climate conditions, especially if risk is averted.

Bettinger et al. (2015) generates near-optimal tree level harvesting plans using heuristic method to maximize the species diversity enabling better ecological stability over time. This significantly increases the *species mingling index* compared to randomly selected trees. To construct this type of detailed harvesting plan in practice, tree level information on species and stem volume is needed. Remote sensing, similar to what is used in this research, can be used to estimate the tree species and volume (Jucker et al., 2017).

2.2 Climate change affecting decision making

The rate of climate change is so rapid that the adaptive capacity of ecosystems is likely not enough to respond to the change leading to local extinction of species and loss of ecosystem services. This introduces novel problems for decision making, as it is not possible to rely solely on historic data for predicting future outcomes. Instead, more stochastic approach should be taken (Bettinger et al., 2013). In addition, it is expected that it may not be entirely possible to control the state and outputs of a forest or other ecosystem through decision making to keep them at current output level (Keenan, 2015).

Keenan (2015) reviews forest management from climate change point of view. He finds that research has focused on predicting the response of species and ecosystems to the climate change, adaptation strategies in forest management and new methods for decision making under uncertainty.

To implement climate change adaptation strategies, clear objectives are needed. For example, possible adaptation methods could be changing either forest structure, species composition or management strategies (Julius et al., 2008). Steenberg et al.

(2011) found that to increase the resistance to the climate change, varying the species composition of harvested trees so that forest age increases, and more resilient species are promoted is the most effective treatment without decreasing the timber supply too much. Different strategies were tested using simulation on different scenarios using the `LANDIS-II` model. In other study by Wintle et al. (2011), the selection of available budget when choosing the adaptation strategy affected the results in a non-linear fashion: with low budget the best strategy is to focus only on reducing forest fires. With a higher budget a mixed strategy to invest also in habitat protection increased the species persistence, since the marginal benefit solely from the fire management was not significant. With even larger budget, spending money on fire management was recommended again. This highlights the need of multiple actions and the need of cost-efficiency analysis when choosing from the set of possible actions.

While it has been popular to assess impacts and risks of the climate change on the ecosystems, it alone does not lead to better management decisions to support adaptation (Keenan, 2015). To better implement adaptation strategies, more focus should be applied to understating social and community attitudes and values that motivate the management of forests. The personal experiences, attitudes and regulation affecting the decision makers should be in line with the climate research. Thus, it is important how the scientific results are presented to decision makers and how they are received. Keenan (2015) emphasizes the importance of collaboration of researchers of different fields, including merging the knowledge of climate and ecosystem sciences with local management needs and indigenous knowledge. In case the decision makers' information and capability of change is lacking, the rising expectations and pressure from the other actors in the society might be developing faster and cause *future shock* for the forest decision makers. This can lead to external and possibly disturbing control of decisions that should be made locally (Kimmins, 2002).

For climate studies, one important aspect is to analyze the amount of carbon stored in a forest. Pukkala (2011) developed a model simulating the carbon cycle in tree growth, decomposition, and harvest products, which allows decision makers to analyze the effects of carbon pricing and distribution of end products. According to the model, the long-term carbon balance of a managed forest is negative (carbon is released) without significant proportion of trees being used in wood products such as planks (long term carbon storage) or as biofuel (which is considered to have zero emissions in legislation, although this assumption has been criticized as too simple, Muench et al., 2013). With improved management where forest sequesters more carbon, the steady state of carbon balance is zero, as the amount of biomass will not grow anymore and the carbon decomposing from the products equals the carbon stored in the new products.

2.2.1 Continuous Cover Forestry

Continuous Cover Forestry maintains continuous uneven-aged forest structure to provide more resilience to varying conditions and stable economic output, although it requires more frequent management interventions than traditional clear-cut approach (e.g. Gaulton, 2010). Especially during the transformation from clear-cut approach, up-to-date inventory data is required (Bennett et al., 2020) to create suitable openings for seedlings to grow (Gaulton, 2010). However, traditional stand-level measures such as average tree height are not suitable anymore (Keefe et al., 2022) as more detailed data is needed. In general, the use of detailed data to make site-specific tactical and operational decisions that consider sustainability is called *precision forestry* (Dash et al., 2016).

Individual tree level data can be used to generate detailed harvesting plans, where decisions are based on tree level inventory that takes variability within a stand and possibly even local climatic and topographic factors into account instead of stand-level averages. In this way, the growth of certain species can be supported by giving more space for them, for example (Keefe et al., 2022). Utilizing tree level information can also notably improve the expected economic value of harvesting (West et al., 2021).

Many silvicultural treatment plans can be complex, have multiple objectives and may require analysis on large spatial areas. With ITD data, decision processes that are usually done in the field during harvesting can be automated so that goals such as tree growth and nature regeneration can be optimized by considering individual tree and geographical values from large area (Keefe et al., 2022).

As another example, knowing the stem spatial pattern allows to optimize the harvester trails to account for preferences in species to be harvested, trees to be harvested for trails and preferring unproductive soil for trails. In addition, as many sustainability certification programs require chain-of-custody documentation, verifiable individual tree level data about the origins of the stems may be desired (Keefe et al., 2022).

However, the usage of individual tree level data has not yet been used as much in operational forestry than it is in research purposes. The usage is still in experimental stage although commercial LiDAR and ITD datasets have become available (Keefe et al., 2022). More research on utilizing ITD data on silvicultural treatments is needed, for example to support autonomous harvesting in the future.

In Finland, major focus has been applied to the managed peatland forests, as they release significant amount of carbon into the atmosphere and nutrients in the water courses. As another example of *ecosystem modeling*, the `SUSI` model has been created for detailed analysis of drained peatland forests (Laurén et al., 2021). It models hydrology, biogeochemical processes and tree stand growth in two-dimensional cross-section between two parallel ditches. It can be used to analyze the effects of controlling water table level by managing ditches, effects of different fertilization schemes and to simulate effects of continuous-cover forestry on peatland forests, as there currently is lack of experimental data on those.

2.3 The utilization of remote sensing data

Using satellites, airplanes, and UAVs such as drones, usage of remote sensing for ecological analysis has become more advanced as the spatial resolution has increased in all of the three sensor carrier types. Sensors capturing RGB, multi- and hyperspectral data as well as radars and laser scanners provide data for various ecological analysis.

One major aspect in UAV remote sensing is *Structure from Motion* (SfM, Schonberger et al., 2016) which is a technique for automatic generation of 3D models and *digital aerial photogrammetric* (DAP) point clouds from overlapping images without prior altitude information. For forestry, this allows the estimation of vegetation height and thus segmentation of individual trees, when the resolution is sufficient (Surový et al., 2019). However, in practice some level of ground altitude information is needed for georeferencing the data.

In addition to SfM, another popular method for acquiring structural data is *aerial laser scanning* (ALS). ALS results in point clouds, and as laser pulses have better penetration capability through leaves, it provides more detailed structural information on trees especially below canopy. Better estimations of topography, stem volume and biomass can thus be generated with ALS. However, SfM can generate equally good estimates on height and crown diameter, and the data acquisition is generally cheaper with SfM than ALS (Laurén et al., 2021). In addition, as standard RGB, multispectral and hyperspectral sensors are used to generate DAP point clouds, the spectral data can be used for assessing tree health or to identify the species (Surový et al., 2019). Multispectral data contains multiple narrow bands, e.g. red, green, blue, red-edge and near-infrared, whereas hyperspectral has more contiguous bands over large spectral range (Veys et al., 2017).

The main output of these DAP point clouds is the *Canopy Height Model* (CHM). It can be used to assess tree height or growth when run regularly. With ground truth data from field surveys, it can be used in regression models to develop estimates for different tree inventory variables, such as diameter at breast height (Goodbody et al., 2017).

Analysis on remote sensing data can be performed on different levels. On *individual tree level*, analysis is often called *object-based analysis*. The objects, here tree crown segments, have features consisting for example height, diameter, and spectral features such as mean NDVI value or RGB intensity. Object-based analysis can be used for example in classifying individual tree species. This is contrary to *pixel-based approach*, which is more sufficient for analyzing rougher data, such as segmenting satellite images to different land cover types (Blaschke, 2010). In addition, the term *area-based analysis* is used when estimations are made for certain homogeneous area, e.g. biomass volume per hectare in certain forest type (Næsset, 2002).

2.3.1 Object-based analysis

To perform analysis on individual tree level, tree crowns must be segmented beforehand. There exist numerous different methods for detecting tree locations and segmenting crowns. In the case of dense conifer forest, *local maxima filtering* is a popular choice (see Chapter 3.3 for more details) for detecting the locations. To delineate crowns, the *watershed* (Vincent et al., 1991) algorithm has traditionally been popular.

As an example of segmentation methods, Luca et al. (2019) has used *Large Scale Mean Shift* (LSMS) algorithm (Michel et al., 2015) for segmenting individual tree crowns. LSMS is a non-parametric iterative clustering method. It can use spectral separability in various layers, like RGB and different Vegetation Index rasters such as NDVI, in addition to Digital Elevation Model layer containing height information. In the study, Random Forest and Support Vector Machine are used for species classification in cork oak woodlands to identify trees, shrubs, grass, soil, and shadow areas from the segmented data. The best features for classification are NDVI and DEM layers.

2.3.2 Species classification

While it generally has been found problematic to separate species due to their large variation in features within species as well as due to changing external conditions (weather, season), it is possible to classify species into a few classes. For example, it is possible to distinct between conifer and deciduous trees as well as healthy and unhealthy trees. Although difficult, species classification needs to be run very rarely after successful survey as forest composition changes slowly (Surový et al., 2019).

Instead of using a specified feature set, deep learning models that find the most important features unsupervised show potential in species classification. Instead of using only spectral averages, deep learning models rely more on spatial structure such as branching pattern and foliage shape of the crowns. For example, Onishi et al. (2021) use four different convolutional neural networks available in `PyTorch` and compared their performance to Support Vector Machine (SVM) classification for two UAV datasets only in RGB channels. For training deep learning models, each crown segment image is augmented eight times by rotating and mirroring the image. For image set taken in autumn where different species have distinct colors, both neural networks and the SVM performed well with slight advantage to the networks. The differences between the four deep learning methods were minor. For image set taken in summer, where leaf colors were more similar to each other, the neural networks performed considerably better than the SVM. When classifying seven species, the convolutional networks at best have an accuracy over 90% whereas the SVM performed only with an accuracy of 70-80 %. These results can be thought as good especially since only segmented RGB images are used without any height data, as usually multi- or hyperspectral data is beneficial for species classification (see for example Nevalainen et al., 2017).

2.3.3 Thermal analysis

There exist some studies also on thermal remote sensing for the purposes of tree health assessment. During an infection, invasion of insects or a drought, one way how trees show stress is stomatal closure. Stomata controls the transpiration of water and intake of CO_2 (Agurla et al., 2018). Stomatal closure causes the leaf temperature to increase, which can be detected using remote sensing (Lindenthal et al., 2005). For example, Smigaj et al. (2015) use a thermal camera sensor equipped on a drone to measure average canopy temperature on trees affected by Red-Band Needle Blight infection. Moderate positive correlation with sub-degree change in canopy temperature was found. With this precision, effort needs to be taken in calibrating the sensor as the recorded values change over time. Along with transpiration rates, environmental factors such as air temperature, wind speed and sun radiation affect canopy temperature (Lindenthal et al., 2005).

2.4 The purposes of this research

To analyze possible future scenarios and the potential range of future conditions, detailed understanding of ecosystem responses to climate change is needed. This research develops methods to perform temporal analysis on individual tree level on boreal forest. It combines data from RGB, multispectral and thermal sensors supporting wide range of analysis. This work is part of research in studying the response of individual trees to long drought conditions.

Here the focus in methods is to develop as accurate as possible detection of individual trees by improving widely used local maxima filtering by using height heuristics and the possibility of using two temporally different data sets. In addition, a new method for statistically estimating the total distribution of trees in the study area is used for the first time in practice.

From the remote sensing point of view, the availability of such a wide range of data on individual tree level, especially when the analysis between the two years is possible for each single tree, is rather unique. Especially the availability of forest-scale thermal orthomosaics provides novel possibilities for research.

3 Materials and Methods

This section presents the used methods. First, briefly the pre-processing steps to obtain orthomosaic and Canopy Height Model are presented. The pre-processing is based on Agisoft Metashape commercial software and tools available in `lidR` R-package.

After that, detection of individual tree locations and segmentation of tree crowns are presented. These are based on algorithms published in literature. In addition, novel methods are presented to both filter incorrect trees and to connect tree crowns between two studies performed year apart using the two datasets. Finally, the total number of trees in the study area is estimated using a recently published statistical method by Kansanen et al. (2022).

To present the full workflow, the complete processing and analysis workflow in this thesis is presented in Figure 2 including the used inputs and outputs for each step.

3.1 Data obtaining and the study site

The data used is collected using drone flights at Ränskälänkorpi study site located in Asikkala, Finland. The image acquisition is performed in September 2020 and June 2021 to study the effects of selection harvesting performed in spring 2021.

The site is used to study the effects of continuous cover forestry in boreal peatland forests. At the site, various biological and meteorological variables are measured, such as soil temperature, water level and gas exchange between the ecosystem and the atmosphere using field measurements and two Eddy-covariance towers. The area of interest is around 500 x 500 meters in size and includes three sections: selection harvest, control (old-growth, unmanaged) and clearcut areas which can be clearly seen in the post-harvest images from 2021 (see the orthomosaic in Figure 1).

Figure 1: The Ränskälänkorpi study site in July 2021, after the selection harvesting and clearcutting.

Images were captured using DJI Matrice 210 V2 drone equipped with Zenmuse XT2 for thermal and RGB imaging and Micasense Altum for multispectral images. During a flight, the drone is moving steadily at a constant altitude (typically 100 m) and images are captured at close interval (once per second) to achieve approximately 90% overlap between the images (Leberl et al., 2010).

Ideal weather conditions improve the quality of the resulting point cloud and surface elevation model. To minimize shadows of objects and brightness differences between the images, it is recommended to capture the images during mid-day either with completely clear sky or with thin even layer of clouds. Wind should be avoided so that for example the branches of the trees do not move between the images. For thermal images, the clear sky produces the largest temperature differences between the moist and dry objects as well as objects with different albedo and emissivity.

3.2 Point cloud pre-processing

After a flight, the images captured using a UAV need to be merged. Through pre-processing, a *dense 3D point cloud* of the forest and an *orthomosaic* are obtained. Orthomosaic is a satellite-like view of the study area where all objects look as if they are being viewed from straight above. Using the dense cloud, height value can be assigned to each pixel in the orthomosaic resulting in Digital Elevation Model (DEM).

The pre-processing steps are presented briefly as following.

Agisoft Metashape Professional 1.7.3 is used to perform the pre-processing steps 1-8 (Agisoft LLC, 2021). Metashape was run on Ubuntu Virtual Machine in CSC cPouta computing environment with 14 CPU cores, 112GB of RAM and 1 NVIDIA Tesla P100 GPGPU. Processing steps 9-15 are performed using `lidR` for R language (Jean-Romain et al., 2021) as batch jobs in CSC Puhti supercomputer.

1. **Align photos** Using aerial triangulation and bundle block adjustment, tie points are found between the images and images are matched. Using camera position from drone (location, altitude, camera angle etc.) and camera parameters (focal length, sensor size etc.), sparse cloud is generated, which is a rough 3D model of the area.

2. **Register Ground Control Points** Iteratively georeference the images to real coordinates using Ground Control Points (GCPs) visible in the images, as the GPS location measured in drone is not accurate enough to solely produce accurate projection for the point cloud. The GCP locations are measured using GPS device in the field. After registration, camera alignment is optimized in Metashape.

3. **Clean cloud** Remove obvious outlier points, like noise below ground, both manually and using values of Reprojection Error and Reprojection Uncertainty.

4. **Dense Point Cloud** Generates a detailed 3D model of the study area using

photogrammetry, see the result in Figure 3.

5. **Digital Elevation Model** Using dense point cloud, the heights of all objects are determined.

6. **Spectral correction** For multispectral images, calibrate the reflectance using panels with known reflectance.

7. **Orthomosaic** The images are projected to the Digital Elevation Model surface.

8. **Export cloud** Save cloud as `.las` files in 100 x 100 m chunks.

9. **Spatial indexing** To speed up the processing of the point clouds, create adaptive quadtree over x and y coordinates where cells represent point index intervals within that region. This is done using `LASindex` from lasTools (rapidlasso GmbH, 2021) and saved in `.lax` format

   Further pre-processing is performed using `lidR` package for R.

10. **Re-scale point offsets** Set distance between points to 0.001 meters and remove duplicate points on that scale.

11. **Clip area** Select the region of interest for analysis.

12. **Denoise** Remove below-ground points by removing points estimated to be below the percentile corresponding to ground.

13. **Classify ground points** Using Cloth Simulation Filter, classify points as ground. The point cloud is turned upside down and “cloth” is dropped on top of the ground. Points under selected distance to the simulated cloth are classified as ground.

14. **Normalize heights** To generate Digital Terrain Model (DTM), which represents the ground surface, triangular irregular network interpolation based on Delaunay triangulation is used for areas where there are no points (e.g. under a tree or other object). The height of all points in the dense cloud are then normalized according to the heights in the DTM raster. Due to discrete nature of DTM, all points ending up below height 0 are removed from the cloud.

15. **Canopy Height Model** With the normalized point cloud, the heights of the trees can be acquired. By removing the ground points by setting their height value as 0 we now get Canopy Height Model. To remove small openings in the canopy, pit-free algorithm is used to interpolate the CHM. To remove additional irregularities, smoothing is applied by representing points as a circle with radius of 2 cm.

After the pre-processing, the obtained height models can be used for detection and segmentation of individual trees.

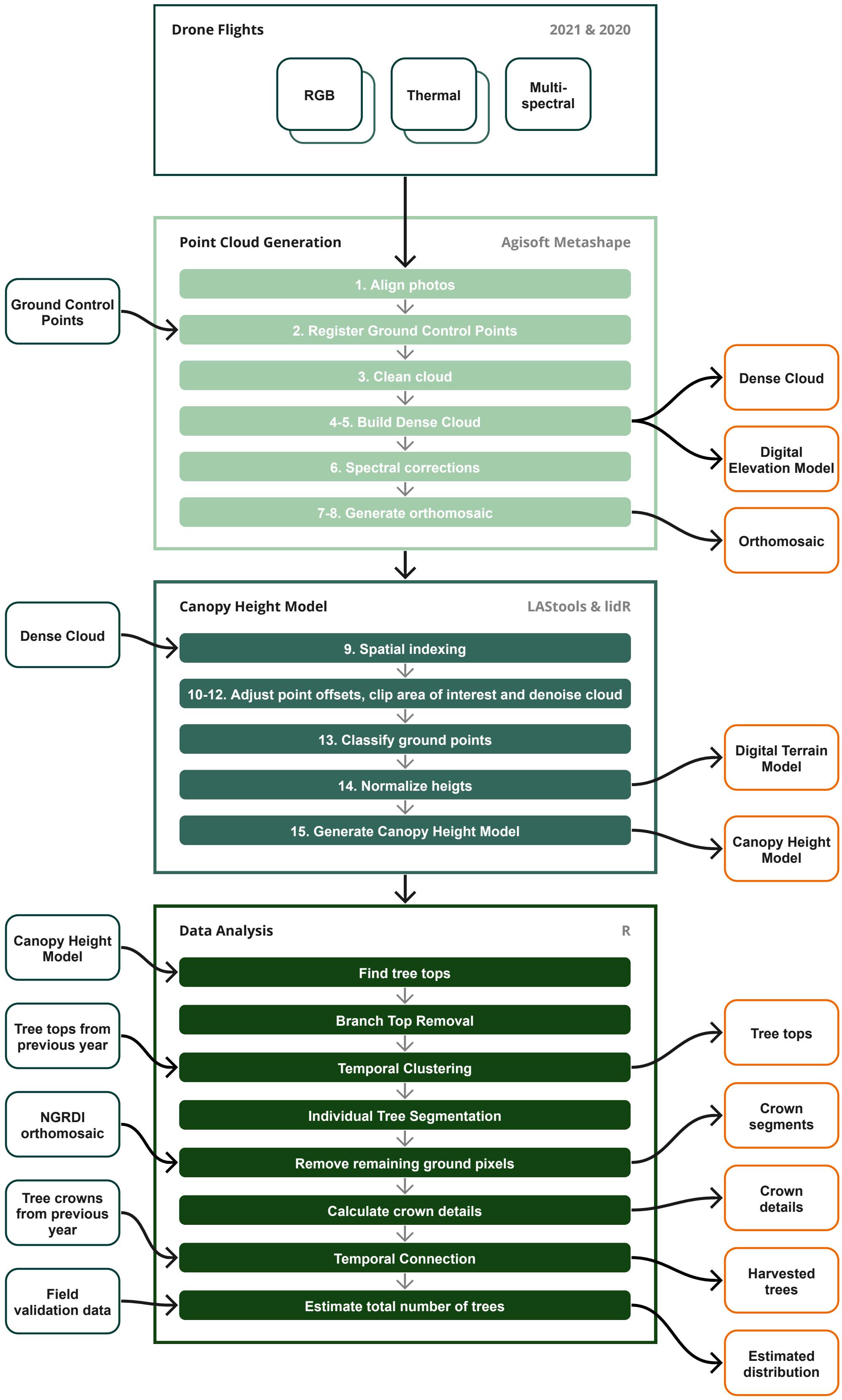

Figure 2: The processing workflow starting the from drone flights

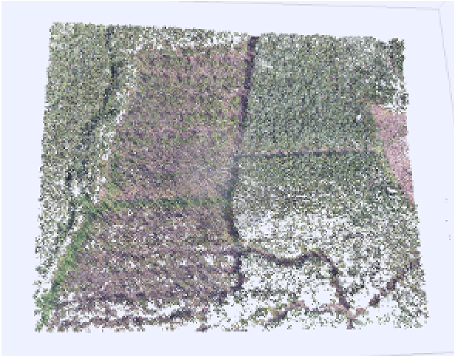

Figure 3: Dense cloud derived from the July 2021 UAV flight. The image on the right is the view from the clearcut site to the edge of the forest in the east of the study area.

3.3 Finding tree locations

The locations of individual trees are identified from the Canopy Height Model using *local maxima filtering* (lmf), which detects unique apex point (tree top) for each tree. Here its used implementation is the `lmf()` function in the lidR-package, which is based on definition by Popescu et al. (2004).

In short, local maxima filtering finds tree tops in locations that have the highest height within a search window. It goes through every pixel in the CHM raster, and if the pixel is the highest within the search window, it is marked as top. Thus, the choice of the search window is important. Popescu et al. (2004) assign different search windows for deciduous and conifer trees according to species classification based on RGB and two infrared channels from the ATLAS satellite. The search windows are modelled based on field measured values of tree crown width and are quadratic models with tree height as the explaining variable. Their resulting search windows vary between 1.5 and 15.5 meters depending on the tree height.

In general, the method suits the best for trees with a single clear apex, like conifer trees. The circle search window was found to perform better than square for deciduous trees, and vice versa. In addition, minimum height threshold is used to not find tops in objects smaller than trees, such as understory vegetation and rocks.

3.4 Branch top removal

An easily occurring problem with the local maxima filtering is that multiple tops are found in the same tree crown, especially when a small search window is used. For example, large conifer crowns typically have tops detected in the end of long branches in addition to the correct apex. This causes problem when estimating the number of stems in the area and also causes incorrectly many tree crown segments as algorithms typically start region-growing from each found top.

To remove these obviously incorrect tops, method that is here called *Branch Top Removal* is used. It examines the neighborhood of each top in the Canopy Height Model. As tree crowns are usually symmetrical, correct tops should lie in the center of the crown with no ground pixels close by. The top is kept if the height difference between the top and the lowest point in its neighborhood is less than a selected threshold. To minimize the disturbing effect of small holes with height value 0 present in the canopy, the CHM is smoothed. The process is presented also in Algorithm 1 and an example of the results can be seen in Figure 4.

Figure 4: Branch Top Removal filters out erroneous tops found using the local maxima filtering algorithm by examining the height differences in the neighborhood of each top.

Algorithm 1 Branch top removal

A $\leftarrow$ set of found tree tops
accepted $\leftarrow$ $list()$
CHM $\leftarrow$ smooth CHM with e.g. 5x5 pixel average

for each found tree top a in A **do**
  Crop circle c with radius r and center point a from the CHM raster
  Get the lowest height in the circle, $h_{\text{min}} = \min(c)$
  if $a_{height} - min(c) < h_{\text{diff}}$ and $a_{\text{height}} > h_{lb}$ **then**
    accepted $\leftarrow$ a
  end if
end for

The method works well especially with conifer trees. For some deciduous trees it leaves multiple tops that visually seem to be in a single crown, but as discussed in

Chapter 4.3, it is difficult to tell solely from the orthomosaic how many individual trunks there actually are.

3.5 Clustering and filtering tops using temporal data

The trees left after the selection harvesting are generally younger and narrower. Notably smaller crowns cause problems for the Branch Top Removal, as the detected apex of a tree is often near the crown edge. As there might be multiple tops detected also for the smaller crowns, some kind of method should be used to remove the incorrect ones. To make matters worse, noise issues in the CHM increase the number of incorrectly detected tops significantly in all areas affected by the noise. Noise points have high height value and are often detected as a top by the local maxima filtering algorithm. Areas in Figure 3 with less points have decreased CHM quality.

As in this study the top detection process is done for the two following years, information from the other year can be utilized to fix the other if it is assumed to be correct. Top locations from the other year can't be used as such, since the orthomosaics have location inaccuracies between them (as discussed in Chapter 4.1) and the selection harvesting done between the surveys has removed large number of trees.

In this case the location inaccuracy, although not entirely uniform, is measured to be less than the average crown diameter. This should allow to match the tops within the two data sets with relatively high accuracy. Particularly, the same process can be used to remove incorrect tops from the 2021 data. Tops in 2021 that are close to single top in the 2020 data are clustered and only one top is left as result. Here the process is called *Temporal Clustering*.

3.5.1 Temporal Clustering

First, for each tree top in the 2021 data, the closest top within a search radius from the 2020 data is assigned. After that, the tops in 2021 with the same closest top are found and the closest one is assigned to be the actual top corresponding the tree. Small enough search radius should be used to prevent wrong tree from distance to be assigned. The detailed method for finding the corresponding tops from the other data set is presented in Algorithm 2.

For selectionally harvested forest, however, the trees visible in the pictures taken after the harvest might be not visible in the earlier data since those trees have been beneath the taller canopy. In other words, finding the exact corresponding post-harvest tree in pre-harvest data is not always possible. However, as the trees in the post-harvest forest are sparse and practically close to some harvested tree, it is still possible to use this method to cluster tops even though not using the actual same tree in pre-harvest data. When generating the actual top pairs in Chapter 3.6, the height difference is considered.

Algorithm 2 Find closest top from the other dataset

$A \leftarrow$ Set of tops with more incorrect tops, here 2021
$B \leftarrow$ Set of tops which is is assumed to be correct, here 2020
$closestToA \leftarrow list()$
$closestToA.distance \leftarrow list()$
$closestToB \leftarrow list()$
$closestToB.distance \leftarrow list()$

for each found tree top a in the set A **do**
    Crop circle c with radius r and center point a of tops from the set B
    if c is not empty **then**
        for each top b_c in circle $c \subset B$ **do**
            $b_c \leftarrow$ distance(a,b_c)
        end for
        $closestToA[a] \leftarrow$ closest top b_c in the set $c \subset B$
        $closestToA.distance[a] \leftarrow$ distance($a, b_{closest}$)
        if $closesTtoB[b] == 0$ or $closestToB.distance[b] > b_{closestDistance}$ **then**
            ▷ Update the closest top for b only if a is the closest to b
            $closestToB[b] \leftarrow a$
            $closestToB.distance[b] \leftarrow$ distance($a, b_{closest}$)
        end if
    else
        ▷ No tops were found from B in c
        $closestToA[a] \leftarrow -1$
        $closestToA.distance[a] \leftarrow -1$
    end if
end for

3.5.2 Filtering tops using clustering

Now incorrect tops can be removed using Algorithm 3 by checking if multiple tops have the same closest top from the earlier year. While removing incorrect tops, it is to be noted that the locations of the remaining top may not correspond to actual tallest point of a tree. Instead, the aim here is to get only single top per one tree crown, so that the segmentation algorithm does not cut the crown into multiple segments. An example of the method is seen Figure 5.

3.6 Generating temporal top pairs

To produce accurate tree-pairs between the pre- and post-harvest datasets, clustering by distance is not enough. As mentioned, the thinning reveals smaller trees under the harvested trees. Thus, the height difference of top pairs should also be taken into account.

Using the Temporal Clustering, Algorithm 3 can simply be extended by adding

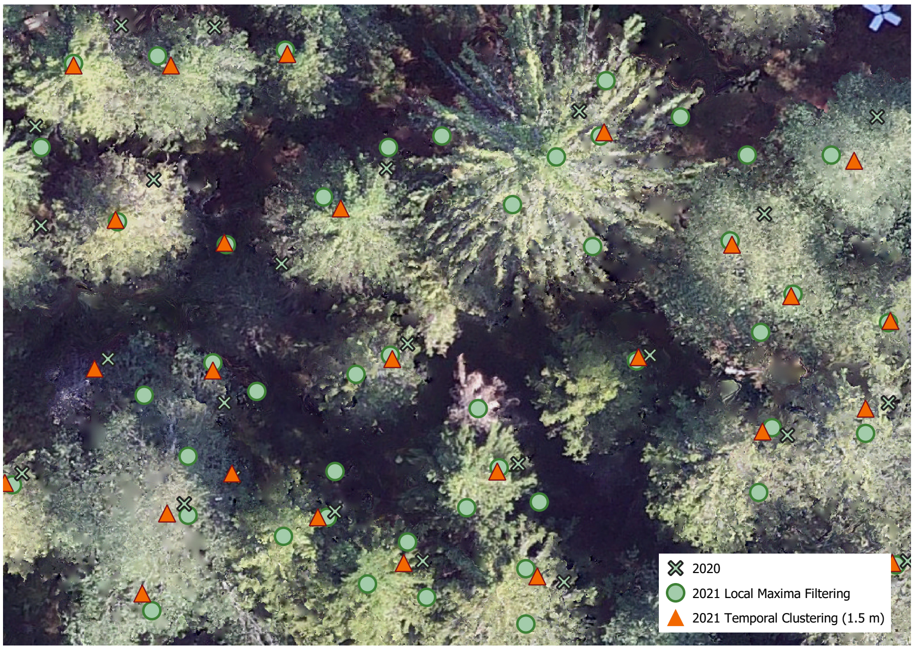

Figure 5: Temporal Clustering filters out erroneous tops using temporal data from the previous measurement. This is especially useful in areas of the CHM affected by noise.

Algorithm 3 Filter tops with temporal information

$A \leftarrow$ Set of tops with more incorrect tops, here 2021
$B \leftarrow$ Set of tops which is is assumed to be correct, here 2020
$filteredTops() \leftarrow list()$
for each found tree top a from the set A **do**
  $b_{closest} \leftarrow$ the closest top for a in B
  $otherTops() \leftarrow$ all tops in A with the same closest top $b_{closest}$
  $a_{main} \leftarrow$ the top in $otherTops()$ with the smallest distance(a_{main},$b_{closest}$)
  $filteredTops() \leftarrow a_{main}$ if not already in the list
end for

check for the height difference of trees. If the CHM has no noise or other significant inaccuracies and the time interval between the surveys is not multiple years for forest to grow significantly, only top pairs with the height difference within a small range (e.g. $[-1, 1]$ meters) should be considered as correct.

An alternative way is to use the crown segmentation obtained in Chapter 3.7. If the two orthomosaics can be georeferenced so that the error in spatial overlap is less than the crown diameters, the crown pairs corresponding to the same tree should have the largest intersection area. So, by calculating the intersection between the crowns from different years and checking for the tree height difference to be minor, a connection can be made. See Algorithm 4.

This *Intersection Method* yields higher accuracy than using the Temporal Clustering method, as it might incorrectly make false connections when two different trees have a distance smaller than the search radius. The Temporal Clustering method, however, could be partly improved by checking the height difference for all trees within search radius and choosing the nearest sufficient. With Intersection Method, the selection of the search radius is not important.

Algorithm 4 Connect tops by maximal intersection

$X \leftarrow$ A set of crown segments, here 2021
$Y \leftarrow$ Another set of crown segments, here 2020
for each found crown $x \in \mathbf{R}^2$ from the set X **do**
    Crop circle c with radius r and center point x of crowns from the set Y
    if c is not empty **then**
        for each crown $y_c \in \mathbf{R}^2$ in circle $c \subset Y$ **do**
            if max(height(x)) - max(height(y_c)) $\in [-1, 1]$ **then**
                $y_c \leftarrow x \cap y_c$
            end if
        end for
        $x_{closest} \leftarrow \max(y_c)$
    else
        $x_{closest} \leftarrow -1$
    end if
end for

3.7 Crown segmentation

The canopy needs to be segmented to individual tree crowns so that all spectral data layers can be delineated as crowns for analysis on individual tree level. The separation of tree crowns is based on found tree tops that should represent the location of apex point of each tree. Here an algorithm working on the Canopy Height Model by Silva et al. (2016) is used for the segmentation.

For each detected tree top, the algorithm first applies a buffer area relative to the tree height that should cover the crown in the CHM. These buffers form a merged polygon, which is split to individual tree crowns using centroidal Voronoi tessellation approach (Sack et al., 1999). Finally, the values of the CHM are filtered by threshold depending on the height of each tree top (Silva et al., 2016). As all ground pixels are marked as 0 in the CHM, the segmentation produces detailed borders around the canopy.

In the `silva2016()` implementation in the lidR package, the algorithm uses nearest neighbor clustering for the Voronoi tessellation. An example of the result is seen in Figure 6.

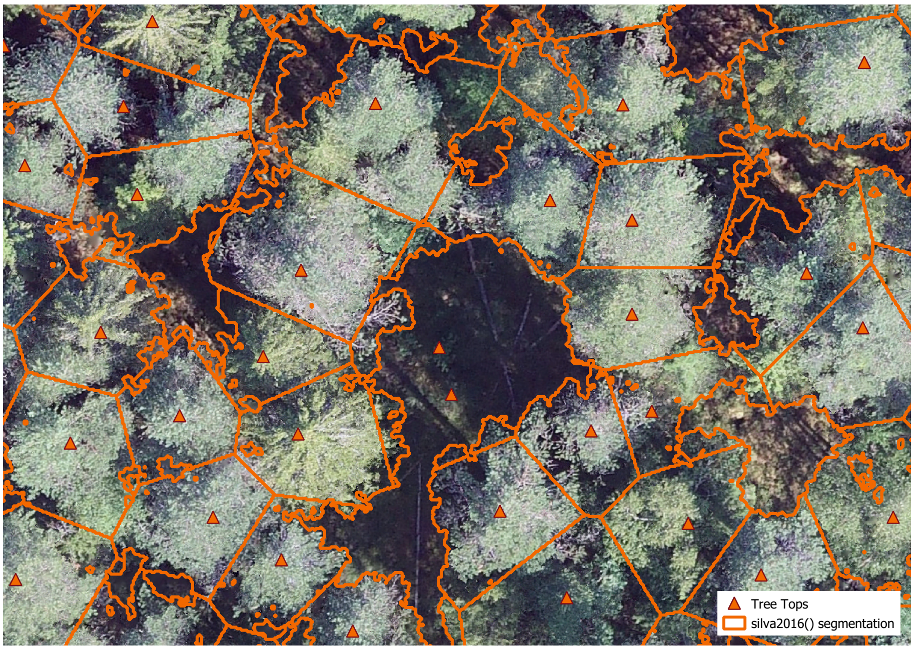

Figure 6: An example of segmentation using the algorithm by Silva et al. (2016).

3.8 Estimating the total number of trees

When using photogrammetric point clouds, trees beneath the crowns of the tallest trees remain unseen. Thus, the number of trees detected corresponds only to the tallest trees and the UAV data needs to be extended in order to perform accurate forest-level analysis with the calculated crown parameters.

One algorithm for estimating the total number of trees in an area is developed by Kansanen et al. (2016). It estimates the total number of trees for those height categories that have been detected using remote sensing. It is based on *germ-grain model*, which is a marked point process model. Here the *germs* are the locations of all objects which are from a random point process. Each object has a attribute, which are referred to as *grains*. In our case, the germs represent locations of the trees and are realizations of homogenous Poisson process with mean λ. The grains represent the crown area as random compact sets with independent, identically distributed areas with random radius R.

Detectability is the probability that uniformly distributed randomly located tree would not be hidden by a larger tree. The parameter $\alpha \in [-1, 1]$ represents the proportion of radius covered by a larger tree where a smaller tree cannot be detected. If positive, the tree is hidden if its center point is located in a set inside the crown of a larger tree. If negative, the set extends the crown and the center point of a hidden tree can be outside of the crown of the larger tree. Detectability can be written for categorized crown radii values $r_i = 1, .., n$ as

$$d_\alpha(r_i) = \begin{cases} 1 - \frac{\left|W \cap [\hat{\Xi}_{R>r} \ominus B(0,\alpha r)]\right|}{|W|} & \alpha > 0 \\ 1 - \frac{\left|W \cap \hat{\Xi}_{R>r}\right|}{|W|} & \alpha = 0 \\ 1 - \frac{\left|W \cap [\hat{\Xi}_{R>r} \oplus B(0,|\alpha| r)]\right|}{|W|} & \alpha < 0 \end{cases}, \quad (1)$$

where $W \in \mathbf{R}^2$ is the whole study area, $\hat{\Xi}_{R>r}$ is the subset of crowns with radius larger than r in the germ-grain model and $B(0,r)$ is the origin-centered closed disc of radius r which models the actual crown. $\ominus$ is morphological erosion for removing a buffer and $\oplus$ is dilation for adding a buffer to the crown (Kansanen et al., 2022). Unlike the original method, here the trees are ordered by the height and not the crown area. The tallest tree in W gets the detectability 1.

When crown radius r is divided into categories, detectability can be thought as sampling probability. The number of trees can be now estimated using *Horvitz-Thompson (HT) estimator* (Horvitz et al., 1952)

$$\hat{N}_{\mathrm{HT}} = \sum_{i=1}^{n} \frac{1}{d_\alpha(r_i)}. \quad (2)$$

Unlike classical HT-estimators, *HT-like estimators* are model-based. The probabilities $d(r_i)$ are estimations and cause bias to the estimate (Kansanen et al., 2022).

The parameter α can be estimated using functional K-nearest neighbors method. With this method, α is optimized using training and validation data. In the case of multiple study areas, first the closest training area i in terms of the similarity of the cumulative size distribution is found for each validation plot j. This is done using Kolmogorov-Smirnov statistic (L^∞) as distance metric. $k \in K$ neighbors with smallest distance d_{ij} are selected for each validation plot j (Kansanen et al., 2022).

Now with the set K, the estimate α_j is obtained as

$$\hat{\alpha}_j = \min_{\alpha \in [-1,1]} \sqrt{\sum_{i \in K} \frac{(N_i(\alpha) - \hat{N}_i(\alpha))^2}{k}}, \quad (3)$$

where $N_i(\alpha)$ is the estimated stand density and $\hat{N}_i(\alpha)$ is the observed stand density in plot i.

Alternatively, α can be estimated for all plots by taking a median of the plot-level values. This is found to be effective strategy by Kansanen et al. (2022). As presented, the number of trees in each height category can now be estimated using Equation (2).

4 Results

In this section, the Individual Tree Detection and Segmentation as well as the estimation of total number of trees and the temporal connection between the two surveys are performed. The goal is to produce statistics for each individual tree crown with the estimated distribution to support further research on the effects of selection harvesting.

This is done by first performing the point cloud pre-processing and analyzing the quality of the results in the Chapter 4.1. Second, the tree top locations that can be assumed to correspond to tree trunk locations are detected, and top pairs between the two temporal data sets are made in Chapter 4.2. The results are compared to field measurements in Chapter 4.3, and the number of total trees is estimated using the HT-like estimator in Chapter 4.4. Third, the crowns are delimited from each other, and the tree level statistics are calculated in Chapter 4.5.

4.1 Point cloud processing

Dense point clouds are generated from the RGB, multispectral and thermal images captured using the drone. The processing workflow using Agisoft Metashape software and lidR R-package is presented in the Chapter 3.2. The output resolutions of the orthomosaics are 2.5 cm/px for the RGB and 12.6 cm/px for the thermal.

Although we obtain a high resolution orthomosaics, the projection of images on the Digital Surface Model suffers from slightly bad quality. RGB orthomosaics suffer from stretching in 2020 and blurriness and noise in 2021, which also affects the CHM, see Figure 8 for examples. While these do not significantly affect the crown segmentation quality in the end, the bad quality projection of images affects the spectral analysis.

For 2021 RGB image set, there are less photos captured and thus less overlap between the pictures in the southern section of the area. This results the dense cloud having a high amount of noise above treetops (see Leberl et al., 2010 and Figure 7). To make the Digital Elevation Model usable, *moderate* noise filtering level is applied in the Metashape when generating the dense cloud (Agisoft LLC, 2021). This, while removing the unwanted noise, reduces the quality and size of the tree crowns especially in the selection harvest area, where the trees are smaller. To overcome the lower quality, *mild* noise removal is used for the selection harvest area. The tree segmentation later in processing is now done twice with CHMs generated from both mild and moderate filtering clouds. This separation in processing for selection harvest and other areas improves the quality of the final segmentation, which is merged from the two.

Another notable source of error lies in GPS accuracy between the measurements done in 2020 and 2021. As it is known that the drone GPS location is not accurate enough itself, Ground Control Points are used to georeference the images and the resulting point clouds. Although GPS accuracy can be significantly improved by

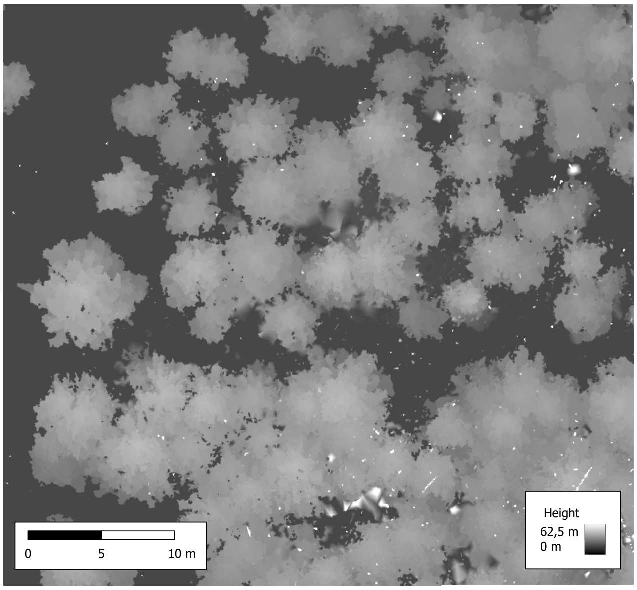

Figure 7: Noise present in the Canopy Height Model due to low image overlap. In this figure, mild noise filtering in the Agisoft Metashape is used.

(a) Stretching issues in 2020 orthomosaic

(b) Blurriness and noise in 2021 orthomosaic

Figure 8: Example of orthomosaic quality issues in the same sample area

using a RTK GPS device on a drone, GCPs are still commonly used to ensure the correct shape of the ground (Stott et al., 2020).

As some of the GCPs were physically destroyed during the selection cutting in early 2021, new ones had to be built and the location of all GCPs were re-measured in summer 2021. This caused unexpected issues: the GPS locations of those GCPs that remained unchanged differed approximately 2-3 meters in latitude and longitude between the 2020 and 2021 measurements. For altitude the difference was up to 20 meters. It is known that the altitude in GPS might be uncertain and that the accuracy may be affected due to trees or other obstacles (Bastos et al., 2013), but higher accuracy was expected. When comparing the 2020 and 2021 orthomosaics, issues with both warping of the CHM and scaling of distances can be seen in the whole area. In other words, for example the location of distinctly the same tree are different in the two datasets. This causes issues for doing temporal analysis, as the georeferencing is incorrect. With for example QGIS Freehand Raster Georeferencer tool, orthomosaics can be aligned, but only locally, as the level of error varies spatially.

The error in location between the two orthomosaics is in the scale of 1 meter. This removes the possibility to do straightforward pixel-level comparison. However, for object-based analysis, like comparing the tree crown objects, the issue can be averted if the crowns can be matched in the different datasets.

4.2 Tree top locations

Tree top detection is based on local maxima filtering, presented in more detail in Chapter 3.3.

The trees in the study site are mostly narrow, but some variation exists in crown size. It can be seen from the RGB orthomosaic that smaller conifer trees have the crown diameter of 2-3 meters while largest deciduous trees have the diameter of 5-7 meters. To find most of the trees, small search window should be used for the local maxima filtering. This, however, generates artificial tops as search diameter smaller than average crown diameter finds tops incorrectly in local maxima, for example in long branches that curve upwards. Small search window can still be used if incorrect tops are removed, as is done in the next sections.

Deciduous trees are often problem for local maxima filtering as, unlike conifer trees, they do not have single apex point but multiple ball-shaped crowns. The use of larger search window for deciduous trees was examined, and for example search window with constant diameter 4 meters could provide better result for some of the deciduous trees. However, it is difficult to interpret which should be the correct number of tops by just using the UAV images without any field measurements, as discussed in Chapter 4.3. In addition, using a different search window for deciduous trees would in practice require identifying the species using some automatic process. As the following methods already remove clear errors from the set of tops reducing the number of total errors, species identification at this stage and species-specific search window was not implemented.

The local maxima filtering is applied using `find_trees()` algorithm from the lidR package. To overcome noise in the CHM, values with height more than 30 meters are maxed at that height, which is approximately the maximum tree height in the site (Figure 11). Minimum tree height is set to be 2 meters, as crowns of saplings are too narrow to be analyzed. Commonly a search window as function of tree height is used (Popescu et al., 2004), but it was noticed that using a constant search window is enough in this case, as the window size is required to be rather small anyway. Using narrower search window at lower heights would detect more objects as tree tops that are not well identifiable as tree crowns in the RGB orthomosaic.

Here constant radius of 1.92 meters is used for normal-sized trees. This finds almost all of even the smallest trees visible, but highly overestimates the number of trees due to incorrect detections. For the trees left after the selection harvest in the 2021 data, radius 2.2 meters is used, since the crowns are more separated from each other and no Branch Top Removal could be applied due to the detected tops being often close to the crown edges. See Figure 9 for an example of the selection harvest area.

Figure 9: Selection harvest area has narrower trees left after the thinning.

4.2.1 Branch Top Removal

Incorrect tops found due to the small search window in the local maxima filtering algorithm can now be removed by examining the neighborhood of each top using the Branch Top Removal presented in Chapter 3.4. The most suitable parameters were found to be search radius $r = 0.65\ m$, tree height lower bound $h_{lb} = 10\ m$ and minimum difference $h_{\text{diff}} = 9\ m$ for 2020. The radius needs to be chosen carefully based on the width of the trees in the site. For 2021 $r = 0.45\ m$ was found to be more suitable due to the quality issues. The Branch Top Removal is applied only to other areas than the selection harvest area, since the tops detected in the selection cutting area are often very near the edges of the tree crowns. To overcome this, temporal filtering is used in the next section.

The effect of this method can be seen in Figure 4, where incorrect tops are filtered out. For the whole study site, most of the incorrect tops are removed in the areas where this method is applicable. On the other hand, remaining areas still have incorrect tops.

To simplify the choice of parameters, the height condition can in this case be simplified to $min(c) > 1$ as the trees have more cylinder than pyramid shape. In other words, simply all tops near ground pixels can be removed.

4.2.2 Temporal Clustering and top pairs

To remove the rest of the incorrect tops, the methods in Chapters 3.5 and 3.6 are used. Here radius of 1.5 meters is used as search window for the top pairs, as the average georeferencing error between the two datasets is approximately less than that. The effect of the method can be seen in Figure 5.

After filtering the 2021 tops by using the 2020 tops only by distance, it is seen in Figure 10b that most of the trees are connected correctly in terms of height difference as 70% of the pairs have difference within -1 to 1 meters. The error is calculated as $h_{\text{diff}} = h_{2021} - h_{2020}$, meaning all connections with significant negative error can be considered incorrect, as trees should not shrink. These cases are mostly in the selection harvesting area (Figure 10a) and correspond to smaller trees revealed below the harvested larger trees. On the contrary, the large number of connections with positive error is not accountable for tree growth either, as annual growth should be within a meter. By visual inspection it can be seen that here those cases are mostly correct connections, and the large difference is caused by the 2021 CHM having incorrectly high noise points.

As a conclusion, only top pairs with height difference within $h_{\text{diff}} = [-1, 6]$ are allowed. The resulting number of total tops from both years and those that did not connect to the other year are shown in Table 1.

The top pair data can be used to find the harvested trees. With the same logic, pre-harvesting tree can be considered as harvested if there is no corresponding top satisfying the distance and height constraints and it lies in the harvested area. The number of harvested trees within the selection harvesting area is 1 740.

For better accuracy, the Intersection Method presented in Algorithm 4 is used for the final top pair result in Chapter 4.5.1.

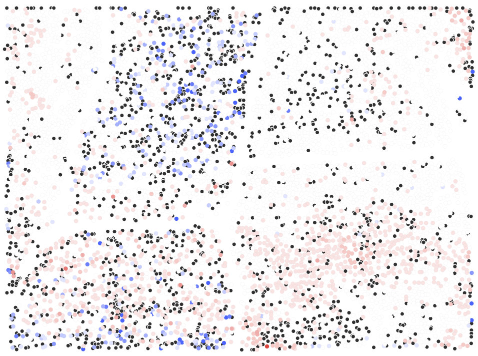

(a) Spatial distribution of the difference. Red: positive difference, blue: negative difference, white: near 0, black: not connected.

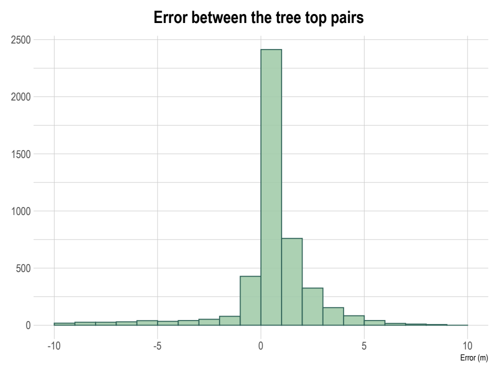

(b) Histogram of the difference.

Figure 10: Difference of height for each 2021 top between a connected 2020 top. Difference is calculated as $h_{\text{diff}} = h_{2021} - h_{2020}$.

Table 1: Number of trees in the final result and number of trees not connected to the data of the other year when cropped to the same extent.

Number of trees	**2020**	**2021**
All trees	7 010	6 289
Not connected (by distance and height)	2792	2085
Not connected (by intersection and height)	2914	1706

4.3 Results and validation to field data

Results of the Individual Tree Detection can be validated using the manually collected field inventory as well as trees detected from the Terrestrial Laser Scanning (TLS). The field inventory is collected in summer 2020 (before the selection harvest) by manually measuring the trees in multiple circle areas. Their location is not precise or at least comparable to UAV ITD, but the inventory can be used to estimate the number of stems in the area and their species distribution.

Individual Tree Detection based on Terrestrial Laser Scanning provides precise locations of stems in two 50 x 50 m survey areas. TLS is performed using scanner located at breast-height, and the resulting point cloud is combined from multiple scans made from different close by locations. The detected trees from the TLS scans have been manually inspected to remove incorrect objects such as measuring devices. Its result can be assumed to be fairly accurate while the most significant error source being close-by or conjoined tree trunks that may have been detected as single trunk.

In some cases, it is problematic to visually tell from the orthomosaic image how many tree trunks there actually are in a crown, especially in the case of deciduous trees which have large crowns. If the forest is sparse enough and the photos are taken at solar elevation angle of ca. 45 degrees, the shadows of the tree trunks give fairly good information about the locations of trunks. See Kattenborn et al. (2018) for example study, where tree trunk diameter is estimated from shadows. For Ränskälänkorpi data sets, this is possible method for the selection harvest area in 2021 data as the area is sparse enough and the trunks cast shadows in the images.

The Figure 11 compares the number of trees with different heights found using the field inventory and the UAV ITD in 2020 data. It is clear that the UAV finds significantly less trees, especially ones with smaller height. This is intuitive as only the tallest trees can be seen from the drone images. It is not possible to visually see beneath the canopy and thus most of the smaller trees with height less than 15 meters are not found in the ITD process.

In addition, some of the larger trees are also missed as it is difficult to estimate the exact number of trunks. Especially with deciduous trees, many of the correct trunks are most likely not detected from the CHM based on drone photos. The result could be improved by using a laser scanner on a drone or other low-altitude vehicle, as the laser pulses can penetrate through the leaves and reveal the location of branches and trunks more precisely (Laurén et al., 2021).

After all, the Improved ITD consisting of methods presented in this study detects larger number of trees than the Baseline solution, which is a plain local maxima filtering using well-chosen search window. This can be seen as good result, since the Baseline solution includes notably larger number of incorrect tops than the Improved version. The presented methods allow the usage of a smaller search window as more tops can be accurately marked as incorrect and can be removed.

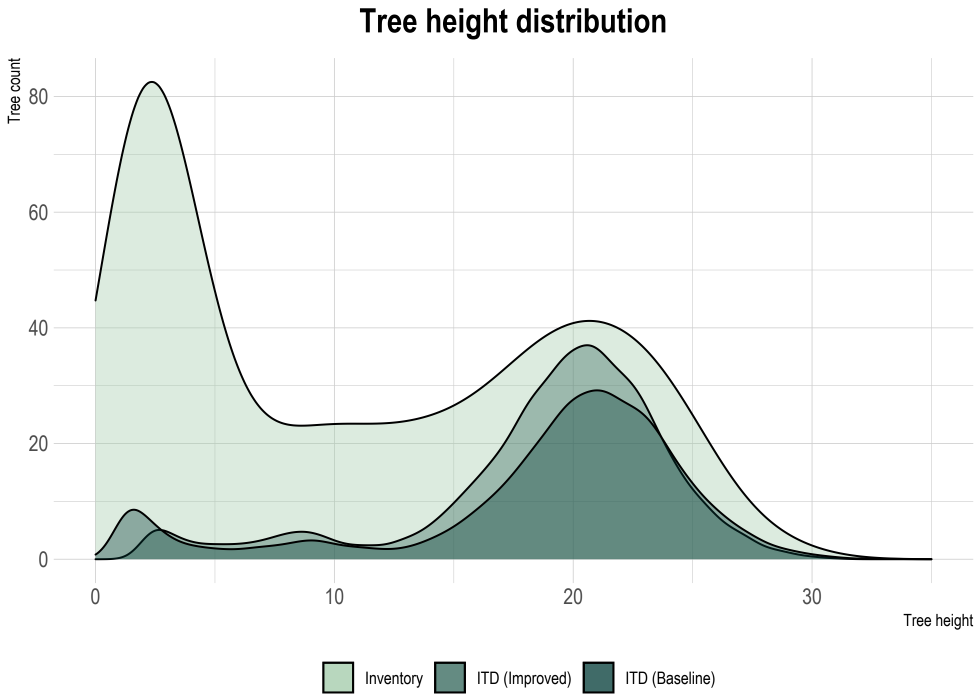

Figure 11: Distribution of trees in the whole study site found using the field survey and Individual Tree Detection from the drone data in 2020 with the Improved (consisting of methods presented in this study) and the Baseline (plain lmf) versions. The number ITD of trees is scaled using the ratio of the approximate area of the field survey and the UAV study area.

When compared to the trees detected using the TLS ITD in Figure 12, the Improved drone ITD detects 54% of the trees in the control site. In more sparse selection cutting site, 80% of the trees are found as most of the trees are visible for the drone. However, the TLS ITD also misses trees with height less than 5 m when compared to the manual field inventory (Figure 11). It can be expected that those trees are present undetected especially in the control area, and their number should be significant. Otherwise, the distributions from the drone and TLS ITD follow similar shape.

While difficult to manually determine exact number of false positives from the thousands of trees in the whole area, in the control area the used methods remove practically all incorrect tops. However, as seen in Figure 12, almost half of the TLS-detected trees are missing. In the partial harvest area, approximately 5% of the found tops are incorrect, while approximately 25% of the TLS-detected trees are missed after utilizing the methods.

As only 54% of the trees in the control area found, in denser forest smaller trees easily remain hidden when viewed from the air. There exist methods to estimate the total number of trees from the UAV data, which allows to overcome the observed bias in the drone survey. One possible method is investigated in the following section.

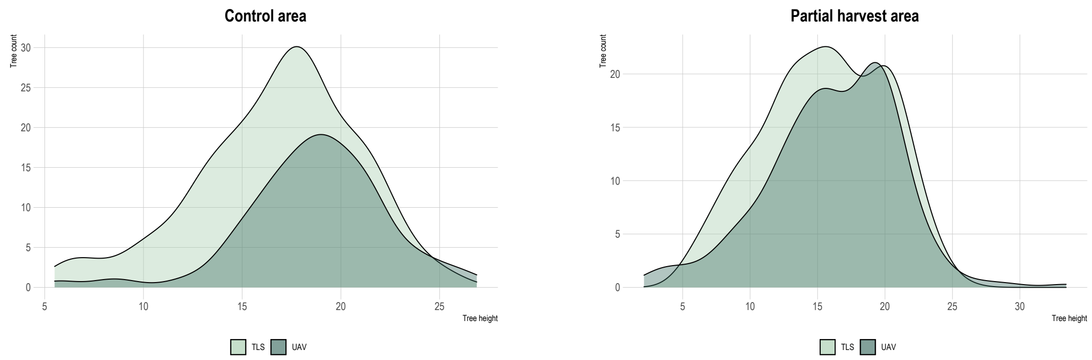

Figure 12: Histogram of trees found using Individual Tree Detection performed on Terrestrial Laser Scanning and drone.

4.4 Estimating the total number of trees

As only the tallest trees can be seen using the drone, smaller trees are left undetected under the topmost canopy layer. One possible method to estimate the total number of trees for the observed height categories is described in Chapter 3.8. It uses training data to estimate detectability $d_\alpha(r_i)$ for each height category of trees detected from UAV images. In other words, the method does not estimate the number of saplings or other smaller trees not visible in UAV images. This is major limitation, since number of them is significant according to the field survey (Figure 11).

The validation data is the individual tree detection performed for the two plots with point clouds from Terrestrial Laser Scans. The training data is the ITD performed on UAV images with a slightly larger area than the TLS point clouds, as whole crowns of the UAV-detected trees need to be included in the set. Here $k = 1$ clusters are used. By comparing the error between observed and estimated number of trees for each α, we find the optimal value of α by numerically solving the root. The values are $\alpha_{\text{harvested}} = -0.299$ for the selection harvest area and $\alpha_{\text{control}} = -0.230$ for the other areas.

When estimating the number of trees for the TLS scan areas, exactly the same number of trunks is obtained with distributions aiming to match the distributions of the trees detected from the TLS (Figure 13). However as seen in Figure 13, the distributions are not equal as some height categories have much higher estimated number and some notably smaller. For many categories, the HT-like estimator is still better than using the UAV ITD value. Inaccuracies in the height category frequencies may cause problems when upscaling the calculated crown parameters for the undetected trees, however.

Now with the site-specific parameter values, the total number of trees in the whole study site can be estimated. When using a slightly smaller area where 5 817 trees are detected from the UAV data, the estimated number of total trees is 9 357. The area is divided into harvest and control (other) areas, and the results in Table 2 follow the same detection rates as for the training areas: in the selection harvest area approximately 80% and in the control area approximately 50% of the trees are detected using the UAV ITD compared to the estimation. As mentioned, the estimation is applied for only the height categories detected by UAV ITD.

Figure 14 shows the distribution of estimated trees and the trees detected from the UAV data for the whole area. When compared to Figures 11 and 12, the HT-like estimation tries to adjust the detected distribution to match the true distribution. However, as the number of TLS-detected trees is small for the smallest height categories, only minor increase in the estimation is applied for those categories.

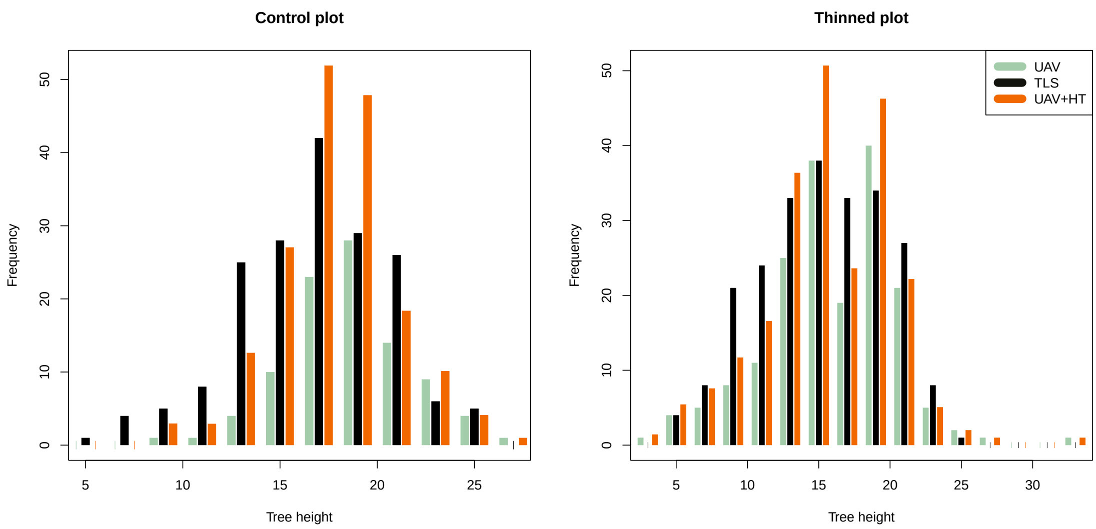

Figure 13: Distribution of HT-estimated trees for control and thinned (selection harvest) survey areas including the trees from the UAV and TLS ITD.

Table 2: Estimated total number of trees obtained with the Horvitz-Thompson -like estimator and trees detected from the UAV data without any estimation for 5 different plots in 2021.

Area #	Type	UAV ITD	HT-like estimation
1	Control	791	1357
2	Harvest	1259	1621
3	Harvest	955	1122
4	Control	1170	2200
5	Control	1642	3057
Total		5817	9357

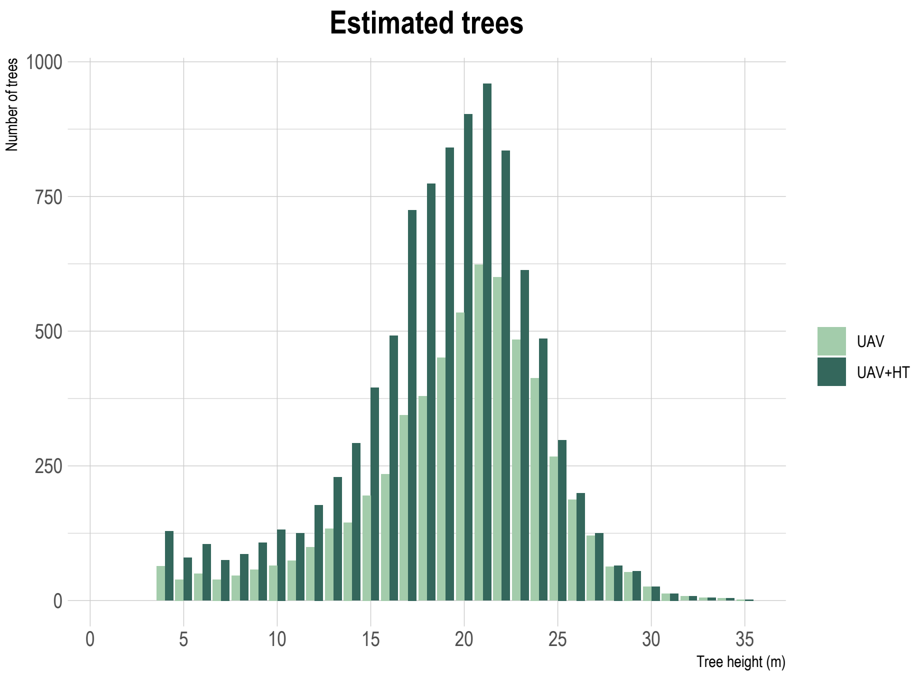

Figure 14: The distribution of trees found using UAV ITD and the estimated number of trees with the HT-like estimator for the whole 2021 data.

4.5 Crown segmentation

With the estimated locations of individual trees, their crowns can now be delineated from the canopy. Here the segmentation is performed using the method presented in Chapter 3.7. To improve the segmentation, all tops with height less than 3 m are removed prior, because their crowns can't be seen from the UAV images in practice.

Due to the noise in the 2021 CHM, the segmentation is done separately for the selection harvest and other areas as more aggressive noise filtering is used for the control area. As the crowns in the selection harvest area are smaller, more aggressive filtering would reduce their size too much. While different noise filtering produces different CHMs, the RGB orthomosaic seems to be mostly the same no matter which version of the CHM is used for the projection.

As the segmentation is based on the CHM, the algorithm delineates the crowns from the ground in detail. However, the segmentation between the trees is rough when the crowns are touching each other (see Figure 15) due to the Voronoi tessellation approach of the algorithm.

In addition, as in some cases the borders of the segmentation might be incorrectly in the crown of another tree, only the largest section actually corresponding to the crown is decided to be kept. This results in more accurate crown details for individual trees, calculated in Section 4.5.2, but as less canopy area is used it gives incorrect value when estimating the total crown area in the study site. In addition, when estimating tree physiology parameters at forest-level, it is slightly different sample than when using all of the crown area, even though the segments might be a bit wrong for individual trees.

After performing the segmentation, there remains some pixels containing understory vegetation or ground due to inaccuracies in the CHM. These can be removed using Vegetation Indices calculated from spectral information, for example NDVI or NGRDI value. Here NGRDI is used, and by manually inspecting the raster, only pixels with $NGRDI > -0.059$ are kept in the crowns. The final result can be seen in Figure 15.

4.5.1 Top pairs using Intersection Method

Connecting the trees between the two flights can now be performed using the Crown Intersection Method explained in Chapter 3.6 with the allowed tree height difference range $[-1, 6]$ as found in Chapter 4.2.2. As a result, common identifier is set for each individual tree in both years. Those trees that are not connected, such as small trees revealed after the selection harvesting, get unique id meaning all ids actually represent separate trees. Now, the temporal analysis of individual trees is possible. In addition, the Intersection Method provides yet another way for removing incorrect tops, or to be more specific, merge crown segments that correspond to the same crown in the other data set.

The resulting tree counts for the Intersection Method are presented in Table 1. For 2021, better results are achieved by leaving most of the smaller trees revealed after harvesting as unconnected. In addition, when multiple segments correspond to the same crown, almost all crown segments now get accurately the correct corresponding top whereas only one of them is taken with distance method. However, inaccuracy in detecting the tops and thus in segmentation increases the number of incorrect connections. For 2020, the missing connections correspond mostly to the harvested trees.

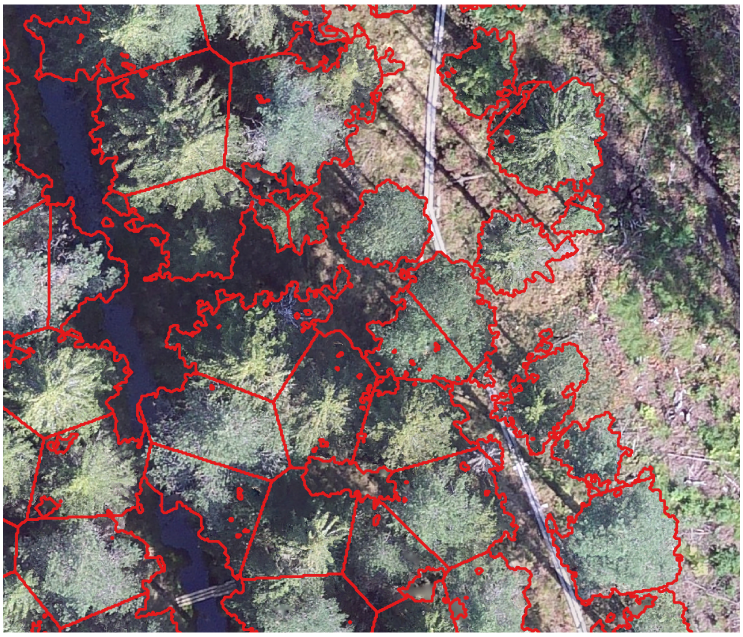

Figure 15: Final segmentation with algorithm by Silva et al. (2016) and NGRDI filtering.

4.5.2 Calculating tree parameters

After the segmentation, parameters in Table 3 are calculated for each individual tree crown. This makes object-based analysis possible for each individual tree.

In our case, the images were captured on a bright day. This caused some number of overexposed (clipping) pixels, in other words, pixels with maximum value 255 in at least one of the RGB channels. For those pixels the exceeding information has been lost. This affected only 6% of the crowns, and the number of clipping pixels is mostly low as seen in Figure 16.

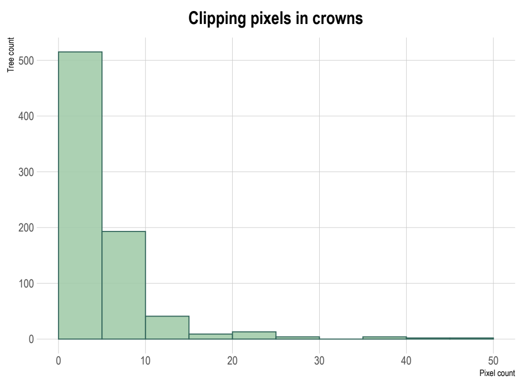

Figure 16: Number of overexposed pixels in crowns having values capping at maximum RGB value.

Table 3: Parameters of each crown

Parameter	**Description**
Crown area [m^2]	Number of pixels in the crown times the image resolution squared
Crown diameter [m]	Average and maximum distance from the tree top to crown edges multiplied by 2. In the most cases the top is near the center point of the crown.
Tree height [m]	Highest point and mean of the top 10% in the height are calculated from the CHM inside the crown.
RGB Intensity [DN]	The mean intensity of the red, green and blue channels of the crown.
NGRDI	Mean of the Normalized Green Red Difference Index, calculated as $$NGRDI = \frac{Green - Red}{Green + Red}.$$
RGBVI	Mean of the Red Green Blue Vegetation Index (Bendig et al., 2015) $$RGBVI = \frac{Green^2 - Red * Blue}{Green^2 + Red * Blue}.$$
NDVI	The mean Normalized Difference Vegetation Index value of the crown from multispectral orthomosaic $$NDVI = \frac{NIR - Red}{NIR + Red}.$$
Temperature [°C]	The mean temperature value of the crown from thermal orthomosaic.

5 Discussion

5.1 Remote sensing

This thesis presents workflow for modern remote sensing relying on point clouds derived from drone photographs using Structure from Motion technique. This provides cheaper alternative to airborne laser scanning using mostly off-the-shelf equipment as well as commercial and open-source software. While not used, there also exists open-source tools for photogrammetric processing of UAV images.

The novel features of this work are the combination of data from RGB, thermal and multispectral sensors, as well as utilizing large temporal data from pre- and post-harvest surveys, which is uncommon for the Boreal region. When merging temporal data, the need for precisely measured drone or Ground Control Point locations is emphasized as fixing the incorrect georeferencing afterwards using image transformations is not possible at this scale. In addition, the selection harvesting caused its own trouble as the remaining trees are notably thinner.

Although point cloud pre-processing requires multiple steps, and especially Ground Control Point registration requires manual work, the process is still mostly automatic. However, as it was noted with the collected data, considerable amount of manual work to ensure the best possible results might be required and multiple error possibilities exist especially during the field surveys.

Although the drone data acquisition is relatively inexpensive, obtaining optimal results is highly dependent on local weather conditions and camera settings. Either clear sky or thin even layer of clouds is the optima for image capturing since changes in radiation affect the analysis especially in the case of thermal sensing. In addition, wind causes the branches to move making the SfM process more difficult (Agisoft LLC, 2021). Moreover, currently the flight times of drones are between 20-40 minutes with one set of batteries. This limits the survey areas as batteries need to be changed during the flight. Image overlap was also remarkably important, as here simply having less image overlap in certain area caused significant amount of noise when constructing the Digital Elevation Model from the photographs.

5.2 Individual Tree Detection and Segmentation

It is a difficult task to find the locations of tree tops and produce crown segmentation with high accuracy. In general, the Individual Tree Detection results achieved here can be considered good when compared to literature (for example Duncanson et al., 2014). With the selection harvest area in 2021, we obtained 80% of the trees detected by the Terrestrial Laser Scanning. For the more denser control area, 54% of trees were found using the UAV methods. The segmentation has sufficient quality for the purposes of the detailed tree physiology analysis. Ground pixels can be well removed from the crown segments using NGRDI value, which is important for calculating any spectral values. However, the delineation of touching crowns could be improved.

In this case, the largest error source for the segmentation are the remaining incorrect tree tops. As the segmentation method starts region-growing from each top, all tops will be assigned its own segment. As incorrect tops may lie in very wrong places (like in seemingly invisible trees between canopy), the resulting incorrect segments might extend partly to correct trees. This is the main reason why such an effort was spent on removing the incorrect tops. In this sense, slightly bigger search window for the local maxima filtering could provide less incorrect tops, especially if the filtering methods presented are applied. In addition, the segmentation and crown details could be used for species classification for different search windows, and heuristics to merge the segments could possibly be developed to include the deciduous trees better. However, in practice it was found the deciduous trees were not more problematic than the other trees.

The algorithm used here for the segmentation by Silva et al. (2016) is rather simple. As characteristic to the central Voronoi tessellation, the touching tree crowns are separated by straight polygon lines. As here it is implemented simply by using K-means clustering on the CHM, any further heuristics or usage of spectral layers for the clustering could improve the results. Speculatively, the Large Scale Mean Shift algorithm (Michel et al., 2015) provides spectral segments that could be clustered as crowns.

Already in `lidR` package and especially literature, there exists many other methods for segmentation and tree detection. Vauhkonen et al. (2012) compares different ITD algorithms (for LiDAR point cloud data). It was found that the performance of the algorithms is similar and that the forest structure has the largest effect on the accuracy. As another case example, Wagner et al. (2018) uses image processing methods to delineate crowns solely from RGB satellite image with 0.5 m pixel resolution.

In addition, there exist some examples of using Convolutional Neural Networks for Individual Tree Detection, like Santos et al. (2019) and Weinstein et al. (2019). Zhou et al. (2020) used more advanced method by using holistically nested edge detection network for tree edge detection and minimum spanning tree method to merge weighted crown segments. These methods show promising accuracy. However, the used method was chosen for practical reasons as it was easily available in the package and the computation time was sufficient.

Especially when using point clouds from Structure from Motion, smaller trees remain unseen beneath the canopy of largest trees. This can be seen well in Figure 11, where the number of trees under 5 meters measured in the pre-harvest field inventory is very high. Although saplings and other small trees remain problem, using airborne laser scanning would generally detect more trees, as the laser pulses penetrate through leaves. For area-based metrics, the number of smaller trees can be statistically estimated using field-data samples, similar to what was done here for the taller height groups (e.g. Kukkonen et al., 2021).

The HT-like estimator used here provides a way to correct the bias in the Individual

Tree Detection and allows to upscale the obtained crown parameters for larger proportion of the actual trees in the site. The estimation procedure clearly makes the distribution more accurate, but it does not consider the smallest tree heights. In case the number of the unobserved height categories would be estimated using some other method, the tree physiology parameters should be estimated using allometric models (Jucker et al., 2017).

5.3 Applicability for decision making and ecosystem modeling

This type of detailed UAV data (with resolution more than 5 cm) is suitable especially for studying ecosystem behavior. For forestry needs, rougher spatial resolution has traditionally been used, but new tree level harvest plans in precision forestry benefit from more detailed data. However, as it was noted in this research, obtaining good quality data using drones is not trivial and the survey areas might be inconvenient for larger forest inventories with current flight ranges. For commercial purposes that may not need such a high-quality data as scientific research, effort should be focused on regularly produced national laser scanning databases which have increasingly high resolution and are already available.

In this case, the data is being used for studying the effects of selection harvesting as well as extreme drought in summer 2021. Temporal data including thermal measurements from 2020 can be used as reference data, and as the analysis is performed on individual tree level, the behavior of individual trees could potentially be considered. In addition, field-measured sensor values such as tree water flow can be estimated for the rest of trees with no sensors installed.

Another focus area, improving the individual tree detection for SfM point clouds, could potentially lead to better estimation for the number of tree size and species categories. This could potentially lead to better estimation of forest inventories, forest biomass, or carbon stored in the site, for example, with minimal amount of field work.

In terms of climate change and biodiversity loss, this type of research helps to analyze ecosystem behavior and generate e.g. harvesting strategies that minimize the ecological impact of silvicultural actions. In general, the possible rapid change in climate conditions needs to be considered when studying ecosystem behavior or refining management strategies for long term. As noted by Keenan (2015), the societal aspect and local communication is major factor when increasing the sustainability and resilience of forests. In addition, the more advanced forestry research has mainly focused on northern and western countries (Keenan, 2015), but the increase in commercially available remote sensing devices such as drones and the availability of open-source software provide possibilities for more research.

6 Conclusion

In this study, an end-to-end process for versatile use of remote sensing data to study the effects of continuous cover forestry is presented. In addition, methods to remove incorrectly detected trees for the Individual Tree Detection are developed and a novel method to statistically estimate the distribution of all trees in the study site is utilized.

By combining RGB, thermal and multispectral data captured using a drone as well as height information derived from the photos using Structure from Motion technique, all visible tree crowns in the forest are segmented and various ecosystem modeling studies for understanding the ecosystem response to changing conditions can be performed. Additionally, the data can be used to support decision making on precision forestry. The drones provide cost-effective and easily scalable process for gathering remote sensing data with processing workflow that requires manual input only on a few steps.

For individual tree level analysis, methods to improve the Individual Tree Segmentation are presented. Commonly used local maxima filtering for tree top detection is extended using two methods for filtering incorrect tops. Branch Top Removal examines the neighborhood of each top to find ones with large height differences suggesting location not at the real apex of the tree. Temporal Clustering takes advantage of the two available data sets from the same study area and overcomes noise issues present in the other by clustering all tops corresponding to the same tree. In addition, temporal data is used to form top pairs between the two surveys and to analyze the number of trees between and after the harvest. As a result, larger number of trees with less false positives is detected compared to a baseline solution of using only local maxima filtering.

For validating and analyzing the results, detailed field survey and ITD performed on Terrestrial Laser Scanning data is used. Particularly, the TLS data is used to statistically estimate the total number of trees in the whole study site by generating model for the detectability of each tree height category found using the drone ITD. For this, Horvitz-Thompson -like estimator is used. This allows to estimate the crown parameters for those trees not detected using the drone.

Combining different types of remote sensing data from Unmanned Aerial Vehicles, planes and satellites to manual and automatic field measurements, detailed analysis of forest ecosystems can be conducted even on individual-tree level. Remote sensing data can for example be used to monitor the health and growth of individual trees. As forests are key factor in nature ecosystems and provide multiple important ecosystem services, understanding forest health as well as interconnections and feedback-loops between other nature and climate systems is crucial.

In general, forest industry benefits from operations research in generating harvest plans, like optimizing structure and species composition to be resilient to varying climate conditions by specifying individual trees for harvesting and choosing harvesting times to obtain maximal economical value by selecting species and size distribution of the timber. Especially in the case of Continuous Cover Forestry, which particularly in the context of managed peatland forests has smaller impact on nature, individual tree level data can be used to optimize the obtained economic and environmental value.

In the future, more research is needed in how to implement individual tree level data on day-to-day forestry operations to enable more sustainable precision forestry. To support this, methods need to provide more detailed data on smaller trees that are currently not detected using airborne remote sensing. This can be done with better statistical estimation from remote sensing data or with novel ground-based sensing methods such as handheld laser scanners. To improve remote sensing results in general, deep learning methods show promising results by providing more accuracy in Individual Tree Detection and Segmentation as well as in species classification tasks.

Climate change adds uncertainty to the decision making, especially as the time scales of forestry are decades and the rate of change in conditions is uncertain. This requires the use of more stochastic modeling, such as Markov decision models, portfolio optimization and stochastic dynamic programming, as decisions cannot be based solely on historic data. It is also important to realize the rapid temporal rate of climate change and the need for understanding the systemic context in addition to fine-tuning small-scale systems.

References

Agisoft LLC (2021). *Agisoft Metashape User Manual Professional Edition.* URL: http://www.agisoft.com.

Agurla S., Gahir S., Munemasa S., Murata Y., and Raghavendra A. S. (2018). "Mechanism of Stomatal Closure in Plants Exposed to Drought and Cold Stress". Advances in experimental medicine and biology 1081, pp. 215–232.

Bastos A. S. and Hasegawa H. (2013). "Behavior of GPS Signal Interruption Probability under Tree Canopies in Different Forest Conditions". *European journal of remote sensing* 46(1), pp. 613–622.

Bendig J., Yu K., Aasen H., Bolten A., Bennertz S., Broscheit J., Gnyp M. L., and Bareth G. (2015). "Combining UAV-based plant height from crop surface models, visible, and near infrared vegetation indices for biomass monitoring in barley". *ITC journal* 39, pp. 79–87.

Bennett G., Hardy A., Bunting P., Morgan P., and Fricker A. (2020). "A Transferable and Effective Method for Monitoring Continuous Cover Forestry at the Individual Tree Level Using UAVs". *Remote sensing* 12(13), pp. 2115–2136.

Bettinger P., Siry J., and Merry K. (2013). "Forest management planning technology issues posed by climate change". *Forest science and technology* 9(1), pp. 9–19.

Bettinger P. and Tang M. (2015). "Tree-Level Harvest Optimization for Structure-Based Forest Management Based on the Species Mingling Index". *Forests* 6(12), pp. 1121–1144.

Blaschke T. (2010). "Object based image analysis for remote sensing". *ISPRS journal of photogrammetry and remote sensing* 65(1), pp. 2–16.

Dainelli R., Toscano P., Gennaro S. F. D., and Matese A. (2021). "Recent Advances in Unmanned Aerial Vehicle Forest Remote Sensing—A Systematic Review. Part I: A General Framework". *Forests* 12(3), pp. 327–354.

Dash J., Pont D., Brownlie R., Dunningham A., Watt M., and Pearse G. (2016). "Remote sensing for precision forestry". *New Zealand journal of forestry (New Zealand Institute of Forestry)* 60(4), pp. 15–24.

Duncanson L. I., Cook B. D., Hurtt G. C., and Dubayah R. O. (2014). "An efficient, multi-layered crown delineation algorithm for mapping individual tree structure across multiple ecosystems". *Remote sensing of environment* 154, pp. 378–386.

Evans C. D., Peacock M., Baird A. J., Artz R. R. E., Burden A., Callaghan N., Chapman P. J., Cooper H. M., Coyle M., Craig E., Cumming A., Dixon S., Gauci V., Grayson R. P., Helfter C., Heppell C. M., Holden J., Jones D. L., Kaduk J., Levy P., Matthews R., McNamara N. P., Misselbrook T., Oakley S., Page S. E., Rayment M., Ridley L. M., Stanley K. M., Williamson J. L., Worrall F., and Morrison R. (2021). "Overriding water table control on managed peatland greenhouse gas emissions". *Nature* 593(7860), pp. 548–552.

Friend A. D., Valentini R., Aubinet M., Matteucci G., Heinesch B., Ciais P., Allard V., Soussana J. F., Manca G., Schulze E. D., Viovy N., Loustau D., Ourcival J. M., Papale D., Bernhofer C., Knohl A., Buchmann N., Grünwald T., Krinner G., Granier A., Seufert G., Ogée J., Carrara A., Miglietta F., Chevallier F., Friedlingstein P., Reichstein M., Keronen P., Noblet N. D., Rambal S., Pilegaard K., Vesala T., and Sanz M. J. (2005). “Europe-wide reduction in primary productivity caused by the heat and drought in 2003”. *Nature* 437(7058), pp. 529–533.

Gaulton R. (2010). “LiDAR mapping of canopy gaps in continuous cover forests: A comparison of canopy height model and point cloud based techniques”. *International journal of remote sensing* 31(5), pp. 1193–1211.

Goodbody T. R. H., Coops N. C., Marshall P. L., Tompalski P., and Crawford P. (2017). “Unmanned aerial systems for precision forest inventory purposes: A review and case study”. *Forestry chronicle* 93(1), pp. 71–81.

Horvitz D. G. and Thompson D. J. (1952). “A Generalization of Sampling Without Replacement from a Finite Universe”. *Journal of the American Statistical Association* 47(260), pp. 663–685.

Jean-Romain R. and Auty D. (2021). *Airborne LiDAR Data Manipulation and Visualization for Forestry Applications. R package version 3.2.2.* URL: `https://cran.r-project.org/package=lidR`.

Jucker T., Caspersen J., Chave J., Antin C., Barbier N., Bongers F., Dalponte M., van K. Y. E., Poorter L., and Sterck F. J. (2017). “Allometric equations for integrating remote sensing imagery into forest monitoring programmes”. *Global change biology* 23(1), pp. 177–190.

Julius S. H., West J. M., and Baron J. S. (2008). *Preliminary review of adaptation options for climate-sensitive ecosystems and resources.* U.S. Environmental Protection Agency.

Kansanen K., Packalen P., Lähivaara T., Seppänen A., Vauhkonen J., Maltamo M., and Mehtätalo L. (2022). “Refining and evaluating a Horvitz–Thompson-like stand density estimator in individual tree detection based on airborne laser scanning”. *Canadian journal of forest research* 52(4), pp. 527–538.

Kansanen K., Vauhkonen J., Lähivaara T., and Mehtätalo L. (2016). “Stand density estimators based on individual tree detection and stochastic geometry”. *Canadian journal of forest research* 46(11), pp. 1359–1366.

Kattenborn T., Hernández J., Lopatin J., Kattenborn G., and Fassnacht F. E. (2018). “Pilot Study on the Retrieval of DBH and Diameter Distribution of Deciduous Forest Stands Using Cast Shadows in UAV-based Orthomosaics”. *ISPRS annals of the photogrammetry, remote sensing and spatial information sciences* IV-1, pp. 93–99.

Kaya A., Bettinger P., Boston K., Akbulut R., Ucar Z., Siry J., Merry K., and Cieszewski C. (2016). “Optimisation in Forest Management”. *Current Forestry Reports* 2(1), pp. 1–17.

Keefe R. F., Zimbelman E. G., and Picchi G. (2022). “Use of Individual Tree and Product Level Data to Improve Operational Forestry”. *Current Forestry Reports* 8 (2), pp. 148–165.

Keenan R. J. (2015). “Climate change impacts and adaptation in forest management: a review”. *Annals of forest science.* 72(2), pp. 145–167.

Kimmins J. H. (2002). “Future shock in forestry Introduction: Future Shock and Forestry”. *The Forestry Chronicle* 78(2), pp. 263–271.

Kukkonen M., Maltamo M., Korhonen L., and Packalen P. (2021). “Fusion of crown and trunk detections from airborne UAS based laser scanning for small area forest inventories”. *ITC journal* 100, pp. 102327–102335.

Laurén A., Palviainen M., Launiainen S., Leppä K., Stenberg L., Urzainki I., Nieminen M., Laiho R., and Hökkä H. (2021). “Drainage and Stand Growth Response in Peatland Forests — Description, Testing, and Application of Mechanistic Peatland Simulator SUSI”. *Forests* 12(3), pp. 293–316.

Leberl F., Irschara A., Pock T., Meixner P., Gruber M., Scholz S., and Wiechert A. (2010). “Point clouds: Lidar versus 3D vision”. *Photogrammetric engineering and remote sensing* 76(10), pp. 1123–1134.

Lindenthal M., Steiner U., Dehne H.-W., and Oerke E.-C. (2005). “Effect of Downy Mildew Development on Transpiration of Cucumber Leaves Visualized by Digital Infrared Thermography”. *Phytopathology* 95(3), pp. 233–240.

Luca G. D., Silva J. M. N., Cerasoli S., Araújo J., Campos J., Fazio S. D., and Modica G. (2019). “Object-Based Land Cover Classification of Cork Oak Woodlands using UAV Imagery and Orfeo ToolBox”. *Remote sensing* 11(10), pp. 1238–1260.

Michel J., Youssefi D., and Grizonnet M. (2015). “Stable Mean-Shift Algorithm and Its Application to the Segmentation of Arbitrarily Large Remote Sensing Images”. *IEEE transactions on geoscience and remote sensing* 53(2), pp. 952–964.

Muench S. and Guenther E. (2013). “A systematic review of bioenergy life cycle assessments”. *Applied energy* 112, pp. 257–273.

Næsset E. (2002). “Predicting forest stand characteristics with airborne scanning laser using a practical two-stage procedure and field data”. *Remote sensing of environment* 80(1), pp. 88–99.

Nevalainen O., Honkavaara E., Tuominen S., Viljanen N., Hakala T., Yu X., Hyyppä J., Saari H., Pölönen I., Imai N., and Tommaselli A. (2017). “Individual tree detection and classification with UAV-based photogrammetric point clouds and hyperspectral imaging”. *Remote sensing* 9(3), pp. 185–219.

Onishi M. and Ise T. (2021). "Explainable identification and mapping of trees using UAV RGB image and deep learning". *Scientific reports* 11(1), pp. 903–918.

Popescu S. C. and Wynne R. H. (2004). "Seeing the Trees in the Forest: Using Lidar and Multispectral Data Fusion with Local Filtering and Variable Window Size for Estimating Tree Height". *Photogrammetric Engineering Remote Sensing* 70(5), pp. 589–604.

Pukkala T. (2011). "Optimizing forest management in Finland with carbon subsidies and taxes". *Forest policy and economics* 13(6), pp. 425–434.

Pukkala T. and Kellomäki S. (2012). "Anticipatory vs adaptive optimization in vitro adventitious shoots formation of stand management when tree growth and subsequent ex vitro performance and timber prices are stochastic". *Forestry* 85(4), pp. 463–472.

rapidlasso GmbH (2021). *LAStools*. URL: `https://rapidlasso.com/lastools/`.

Sack J.-R. and Urrutia J. (1999). *Handbook of Computational Geometry*. Elsevier Science Technology.

Santos A. A. D., Junior J. M., Araújo M. S., Martini D. R. D., Tetila E. C., Siqueira H. L., Aoki C., Eltner A., Matsubara E. T., Pistori H., Feitosa R. Q., Liesenberg V., and Gonçalves W. N. (2019). "Assessment of CNN-Based Methods for Individual Tree Detection on Images Captured by RGB Cameras Attached to UAVs". *Sensors* 19(16), pp. 3595–3306.

Schonberger J. L. and Frahm J.-M. (2016). "Structure-from-Motion Revisited". *2016 IEEE Conference on Computer Vision and Pattern Recognition (CVPR)*, pp. 4104–4113.

Sebestyén V., Czvetkó T., and Abonyi J. (2021). "The Applicability of Big Data in Climate Change Research: The Importance of System of Systems Thinking". *Frontiers in environmental science* 9.

Silva C. A., Hudak A. T., Vierling L. A., Loudermilk E. L., O'Brien J. J., Hiers J. K., Jack S. B., Gonzalez-Benecke C., Lee H., Falkowski M. J., and Khosravipour A. (2016). "Imputation of Individual Longleaf Pine (Pinus palustris Mill.) Tree Attributes from Field and LiDAR Data". *Canadian journal of remote sensing* 42(5), pp. 554–573.

Smigaj M., Gaulton R., Barr S. L., and Suárez J. C. (2015). "UAV-Borne Thermal Imaging For Forest Health Monitoring: Detection Of Disease-Induced Canopy Temperature Increase". *International archives of the photogrammetry, remote sensing and spatial information sciences.* XL-3/W3(3), pp. 349–354.

Steenberg J. W. N., Duinker P. N., and Bush P. G. (2011). "Exploring adaptation to climate change in the forests of central Nova Scotia, Canada". *Forest ecology and management* 262(12), pp. 2316–2327.

Stott E., Williams R. D., and Hoey T. B. (2020). “Ground Control Point Distribution for Accurate Kilometre-Scale Topographic Mapping Using an RTK-GNSS Unmanned Aerial Vehicle and SfM Photogrammetry”. *Drones* 4(3), pp. 55–76.

Surový P. and Kuželka K. (2019). “Acquisition of Forest Attributes for Decision Support at the Forest Enterprise Level Using Remote-Sensing Techniques—A Review”. *Forests* 10(3), pp. 273–302.

Vauhkonen J., Ene L., Gupta S., Heinzel J., Holmgren J., Pitkänen J., Solberg S., Wang Y., Weinacker H., Hauglin K. M., Lien V., Packalén P., Gobakken T., Koch B., Næsset E., Tokola T., and Maltamo M. (2012). “Comparative testing of single-tree detection algorithms under different types of forest”. *Forestry* 85(1), pp. 27–40.

Veys C., Hibbert J., Davis P., and Grieve B. (2017). “An ultra-low-cost active multispectral crop diagnostics device”. *2017 IEEE SENSORS*, pp. 1005–1007.

Vincent L. and Soille P. (1991). “Watersheds in digital spaces: an efficient algorithm based on immersion simulations”. *IEEE transactions on pattern analysis and machine intelligence* 13(6), pp. 583–598.

Wagner F. H., Ferreira M. P., Sanchez A., Hirye M. C. M., Zortea M., Gloor E., Phillips O. L., de Souza Filho C. R., Shimabukuro Y. E., and Aragão L. E. O. C. (2018). “Individual tree crown delineation in a highly diverse tropical forest using very high resolution satellite images”. *ISPRS journal of photogrammetry and remote sensing* 145, pp. 362–377.

Weinstein B. G., Marconi S., Bohlman S., Zare A., and White E. (2019). “Individual Tree-Crown Detection in RGB Imagery Using Semi-Supervised Deep Learning Neural Networks”. *Remote sensing* 11(11), p. 1309.

Weintraub A. and Romero C. (2006). “Operations Research Models and the Management of Agricultural and Forestry Resources: A Review and Comparison”. *Interfaces* 36(5), pp. 446–457.

West T., Sessions J., and Strimbu B. M. (2021). “Heuristic Optimization of Thinning Individual Douglas-Fir”. *Forests* 12(3), pp. 280–294.

Wintle B. A., Bekessy S. A., Keith D. A., van Wilgen B. W., Cabeza M., Schröder B., Carvalho S. B., Falcucci A., Maiorano L., Regan T. J., Rondinini C., Boitani L., and Possingham H. P. (2011). “Ecological–economic optimization of biodiversity conservation under climate change”. *Nature climate change* 1(7), pp. 355–359.

Wulder M. A., Bater C. W., Coops N. C., Hilker T., and White J. C. (2008). “The role of LiDAR in sustainable forest management”. *Forestry chronicle* 84(6), pp. 807–826.

Zhou Y., Wang L., Jiang K., Xue L., An F., Chen B., and Yun T. (2020). “Individual tree crown segmentation based on aerial image using superpixel and topological features”. *Journal of applied remote sensing* 14(2), pp. 022210–022225.